

Bulk, molecular and spectroscopic analysis of organic matter reactivity classes isolated
from St. Lawrence estuary sediment

Mina Ibrahim

A Thesis

in

The Department

of

Chemistry and Biochemistry

Presented in Partial Fulfillment of the Requirements

for a Degree of Master of Science (Chemistry) at

Concordia University

Montreal, Quebec, Canada

March 2012

© Mina Ibrahim, 2012

CONCORDIA UNIVERSITY

School of Graduate Studies

This is to certify that the thesis prepared

By: Mina Ibrahim

Entitled: Bulk, molecular and spectroscopic analysis of organic matter reactivity classes isolated from St. Lawrence estuary sediment

and submitted in partial fulfillment of the requirements for the degree of

Master of Science (Chemistry)

complies with the regulations of the University and meets the accepted standards with respect to originality and quality.

Signed by the final Examining Committee:

_____ Dr. Guillaume Lamoureux

_____ Dr. Cameron Skinner

_____ Dr. Xavier Ottenwaelder

_____ Dr. Yves Gélinas

Approved by

Chair of Department or Graduate Program Director

_____ 2012

Dean of Faculty

Abstract

Bulk, molecular and spectroscopic analysis of organic matter reactivity classes isolated from St. Lawrence estuary sediment

Mina Ibrahim, M.Sc

Concordia University, 2012

Marine sediments constitute the major long-term sink for organic carbon (OC) on Earth, with <0.3% of the organic matter (OM) photosynthesized yearly in the global ocean ultimately becoming buried (Hedges and Keil, 1995). Burial of this small fraction of OM plays an important role in the global O₂ and CO₂ cycles, making elucidation of the mechanism controlling OM preservation of great importance. Three major OM fractions with contrasting chemical reactivities have been identified within sediments: labile (degraded in oxic/anoxic conditions), non-hydrolyzable (degraded in oxic conditions), and refractory (preserved in oxic/anoxic conditions). Identification of the reactivity classes, however, remains operationally defined; >75% of sedimentary OM remains molecularly uncharacterized. Bulk, spectroscopic and molecular techniques were used to investigate the mechanistic and chemical effects of physical protection and composition on OM preservation. A chemical fractionation procedure was implemented to separate and quantify OM from estuarine and lacustrine sediments with differing OM sources. Bulk (elemental and isotopic) analysis of the isolated fractions revealed the overall contribution of each class to total OM and any mechanistic relationships that may contribute to preservation. The project then focused on one fraction of particular interest, non-hydrolyzable organic matter (NHOM). Spectroscopic (FTIR and NMR) analysis was used to determine the chemical nature of NHOM. An optimized chemical oxidation utilizing ruthenium tetroxide (RuO₄) was used to investigate the molecular structure,

revealing a composition of cross-linked aliphatics regardless of the OM source. Compound specific isotope analysis of oxidation products suggested a common isotopic makeup of the preserved OM.

Acknowledgements

First and foremost, to my family; their unwavering support and strength has been pivotal to successful completion of this endeavor. Secondly to my supervisor, Yves Gélinas; since accepting me as a volunteer there has been no end to the opportunities given to me by Yves. To my official (and unofficial) LEGO lab mates: Robert Panetta, Alexandre Ouellet, Karine Lalonde, Anja Moritz, Andrew Barber, Andrea Clarke and to the plethora of undergraduate research students and volunteers for the many discussion, help and generally making everything more animated. To Maria Ciaramella and Hilary Scuffell who were very supportive through the years. The captains and crew of the *R/V Coriolis II* are thanked for help with sample collection. Funded by NSERC-Canada and FQRNT-Quebec, with additional financial support from Concordia University.

“You have brains in your head. You have feet in your shoes.
You can steer yourself any direction you choose. You're on your own.
And you know what you know. And YOU are the one who'll decide where to go...”

- Dr. Seuss, *Oh, the Places You'll Go!*

Table of contents

| | |
|---|------------|
| List of Figures | ix |
| List of Tables | xi |
| List of Acronyms | xii |
| Chapter I | 1 |
| GENERAL INTRODUCTION | 1 |
| 1.1. Organic Geochemistry | 1 |
| 1.2 The organic carbon cycle | 2 |
| 1.3 Organic matter preservation..... | 5 |
| 1.3.1 Adsorption..... | 5 |
| 1.3.2 Encapsulation into the mineral matrix | 6 |
| 1.3.3 Geopolymerization..... | 7 |
| 1.4 Non-hydrolyzable organic matter | 7 |
| 1.5 Arrangement of thesis | 9 |
| Chapter II | 11 |
| Abstract | 12 |
| Introduction | 13 |
| Methods | 16 |
| 2.3.1 Sampling sites | 16 |
| 2.3.2 Sampling | 17 |
| 2.3.3 Fractionation method | 18 |
| 2.3.3.1 Solvent extraction | 19 |
| 2.3.3.2 Demineralization..... | 20 |
| 2.3.3.3 Hydrolysis | 20 |
| 2.3.4 Elemental and isotopic analysis | 21 |
| 2.3.5 FT-IR | 21 |
| Results and discussion | 23 |
| 2.4.1. Elemental composition..... | 24 |
| 2.4.2. Isotopic composition..... | 27 |
| 2.4.3 FT-IR | 30 |

| | |
|---|-----------|
| Conclusion and implications | 34 |
| CHAPTER III | 36 |
| Abstract..... | 37 |
| Introduction..... | 38 |
| Methods..... | 40 |
| 3.3.1 Sampling | 40 |
| 3.3.2 NHOM isolation..... | 40 |
| 3.3.3 ¹³ C Solid-state NMR spectroscopy | 41 |
| 3.3.4 ¹ H High-Resolution-Magic Angle Spinning (HR-MAS) NMR spectroscopy | 42 |
| 3.3.5 ¹ H- ¹³ C Heteronuclear Single Quantum Coherence (HSQC) spectroscopy | 42 |
| 3.3.6 Ruthenium tetroxide oxidation..... | 43 |
| 3.3.7 GC-MS and GC-FID analyses | 44 |
| 3.3.8 GC-C-IRMS analyses | 45 |
| Results & Discussion..... | 46 |
| 3.4.1 Abundance of the NHOM fraction..... | 46 |
| 3.4.2 Structural analysis of NHOM | 46 |
| 3.4.3 RuO ₄ Oxidation products..... | 49 |
| 3.4.4 Compound-specific δ ¹³ C analysis (CSIA) of the RuO ₄ oxidation products..... | 54 |
| Conclusion | 59 |
| Chapter IV..... | 62 |
| General Conclusion..... | 62 |
| References..... | 65 |

List of Figures

| | |
|---|----|
| Figure 1.1 Simplification of organic carbon cycle..... | 4 |
| Figure 1.2 %OC profiles obtained through theoretical modeling of diagenesis of different reactivity classes based on their exposure to oxygen (light grey region) generating the combine graph on the right | 9 |
| Figure 2.1 Schematic of the wet chemical fractionation method used to isolate the different reactivity classes..... | 19 |
| Figure 2.2 Contribution of different reactivity classes to (a) total OC, (b) total N, and their (c) C/N atomic ratios, (d) $\delta^{13}\text{C}$ and (e) $\delta^{15}\text{N}$ signatures. Sample numbers correspond to Lake Jean 0-5 cm (1) and 9-15 cm (2); Station DE (3); Station 23 0-5 cm (4) 5-10 cm (5), 15-18 cm (6), 28-33 cm (7); Station 16 0-5 cm (8) and 10-14 cm (9) | 30 |
| Figure 2.3 FT-IR spectra of demineralized samples of surface sediments (0-5 cm) from stations (a) D-E, (c) 23 and (e) 16, as well as for the demineralized + hydrolyzed samples from stations (b) D-E, (d) 23, and (f) 16. The numbers at the top correspond to wavenumbers of interest that are discussed in the text. Each pellet weighed 100 mg with 1% carbon content by weight..... | 31 |
| Figure 3.1 Schematic Solid-state ^{13}C CP-MAS NMR of the fresh, mixed, and salt-water samples..... | 47 |
| Figure 3.2 ^1H HR-MAS (top) and ^1H diffusion edited (bottom) NMR spectra of the fresh (Station DE) and salt water (Station 16) samples. The asterisk corresponds to the locking standard DMSO-d6. | 48 |
| Figure 3.3 ^1H - ^{13}C HSQC of the freshwater surface sample. The aliphatic region (A1) is expanded in the insert. | 49 |

Figure 3.5 The terrestrial vs. aquatic ratio (TAR) shows a clear relationship between chain length preference and distance from the mouth of the SLE for alkanolic acids liberated from untreated sediments and their NHOM residues 51

Figure 3.6 Carbon preference index (CPI) values show a clear difference in the even-to-odd ratios calculated for the untreated samples and their isolates 52

Figure 3.7 The comparison of the $\delta^{13}\text{C}$ stable isotope signature of alkanolic acids liberated from the untreated sediments and their NHOM isolates shows a nearly linear relationship reflecting the variations in relative contributions from terrestrial (lower $\delta^{13}\text{C}$ values) 57

Figure 3.8 Compound-specific $\delta^{13}\text{C}$ stable isotope signatures of the alkanolic acids from (a) the untreated sediment and (b) their NHOM isolates..... 58

List of Tables

| | |
|---|----|
| Table 2.1: Sample location and characteristics..... | 17 |
| Table 2.2: Organic carbon (OC) and total nitrogen (TN) contributions of the different OM fractions to total organic matter, and their elemental and isotopic signatures..... | 28 |
| Table 3.1 Quantification of alkanolic acids from RuO ₄ treatment..... | 53 |
| Table 3.1 (cont.) Quantification of alkanedioic acids from RuO ₄ treatment..... | 54 |
| Table 3.2. Compound-specific δ ¹³ C analysis of the oxidation products from the RuO ₄ treatment..... | 58 |

List of Acronyms

OC: Organic carbon

TN: Total Nitrogen

OM: Organic matter

NHOM: Non-hydrolyzable organic matter

FT-IR: Fourier transform infrared spectroscopy

HR MAS-NMR: High-resolution magic angle spin nuclear magnetic resonance

$\delta^{13}\text{C}$: Stable carbon 13 signature

$\delta^{15}\text{N}$: Stable nitrogen 15 signature

IAEA: International atomic energy agency

SLE: St. Lawrence estuary

CSIA: Compound specific isotope analysis

TAR: Terrestrial-to-aquatic ratio

CPI: Carbon preference index

Chapter I

GENERAL INTRODUCTION

1.1. Organic Geochemistry

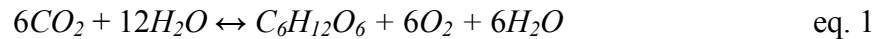
The field of Organic Geochemistry had its beginnings in petroleum chemistry with the identification of organic molecules in coals and oils (Treibs, 1936). Organic geochemistry has since expanded to the study of organic molecules encased in rocks, sediments and soils, focusing on the chemical and biological processes that dictate their formation, as well as the interdependencies and overlays between organic and inorganic matter.

Over the past few decades, it has been shown that the cycling of organic carbon in sediments and soils is strongly intertwined with other elemental cycles - including those of oxygen, nitrogen and sulfur. Geochemists are especially interested in the carbon that is isolated from the organic carbon cycle (Figure 1.1) and retained in sediments and sedimentary rocks over geological timescales (hundreds of thousands of years). This long-term preservation of carbon is the main controller of the concentration of atmospheric carbon dioxide and oxygen and is of interest when considering the origin of fossil fuels (Berner, 2003).

Due to its significant role in maintaining the atmospheric balance of carbon dioxide and oxygen, it is imperative to understand the turnover of organic matter in sediments, starting with its photosynthesis to its ultimate preservation within sediments. These events, summarized below, make up a portion of the global carbon cycle.

1.2 The organic carbon cycle

Sedimentary organic matter (OM) comes from a number of possible sources: terrestrial plants, eroded soils, marine plants and bacteria. Though the photosynthetic origin of sedimentary OM is often ambiguous, photosynthesis itself can be simplified by eq.1, which describes the fixation of carbon dioxide into a molecule of glucose.



Shortly after synthesis (less than 1000 yrs), most of the OM is reoxidized to CO₂ (reverse of eq. 1), usually through bacteria and other heterotrophs. Some OM, however, is not utilized and can eventually sink down to the sediment. Coastal and oceanic waters however are hundreds to thousands of meters deep and fresh OM has a density only slightly higher than that of water (Wagai & Mayer, 2007). Freshly produced organic particles therefore seldom reach the seafloor. Denser biogenic particles like fecal pellets or OM that anchors itself to a denser mineral can however sink quickly through the water column (Fowler & Knauer, 1986).

Even if OM is carried on denser particles, it takes many years to sink through the water column. During this time, OM is partially degraded, reworked and finds stability through mineral adsorption and/or aggregation. These transformations persist once OM is deposited on the seafloor (Ransom *et al.*, 1998). Ultimately, less than 0.3% of the global yearly production of photosynthesized OM is preserved within marine sediments (Hedges & Keil, 1995). Geochemists have attempted to deduce the molecular makeup of sediment OM in order to shed light on the nature of its recalcitrance. The challenge is that the structure of preserved OM is so highly reworked that it becomes difficult to assign it to the class of compound it originated from or even to the organism that originally produced

it. The organic material in sediments is often referred to as molecularly uncharacterized OM because it does not fall into any of the three major biochemical classes (lipid, carbohydrate or protein) and is not identifiable using the most current chromatographic techniques (Hedges *et al.*, 2000). Despite all the difficulties associated with understanding OM recalcitrance, a number of possible preservation mechanisms have been put forth and will be discussed in the following section.

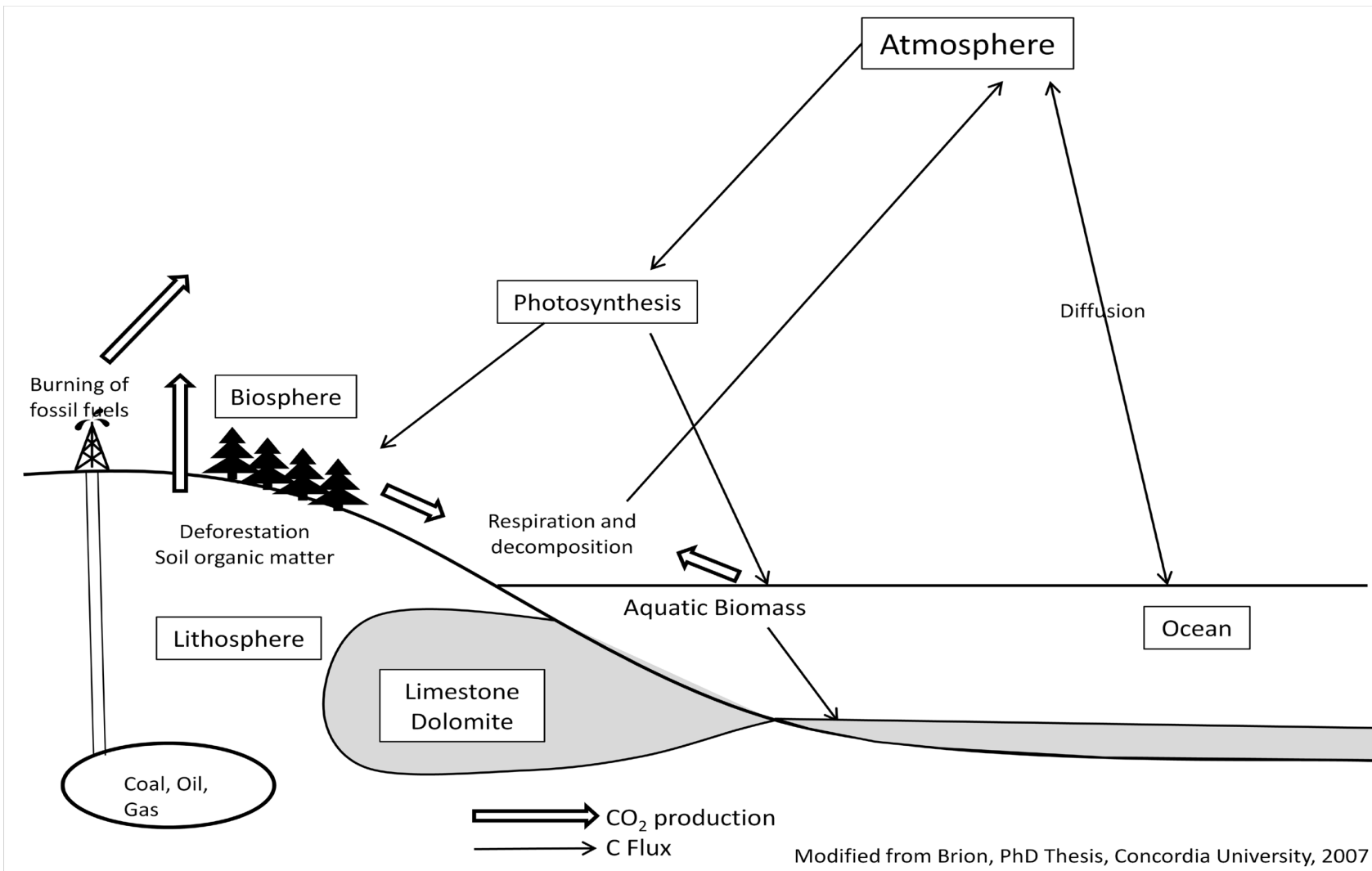


Figure 1.1 Simplification of organic carbon cycle

1.3 Organic matter preservation

Approximately 90% of carbon burial – and preservation - occurs on the continental shelf and in river deltas despite the fact that these areas account for less than 20% of the global area of sediment coverage (Hedges & Keil, 1995). Field data suggests that the depositional environment plays a key role; high sedimentation rates and low concentrations of oxygen in the bottom waters have been linked to high OM preservation, whereas sediments that are continually mixed or resuspended by bioturbation and bottom water currents tend to accumulate little OC (Burdige, 2006). Environmental factors that control carbon preservation vs. degradation of a large pool of OM are difficult to determine on the timescale of a field study or a laboratory experiment since sedimenting OM has a large range of reactivities with half lives ranging from 10 to 2000 years and longer (Hedges & Keil, 1995). Besides the depositional setting, other factors have been suggested as potential preservation mechanisms within sediment OM including 1) adsorption to the mineral matrix, 2) encapsulation into the mineral matrix and 3) geopolymerization of sediment OM.

1.3.1 Adsorption

More than 90% of the organic matter in sediments has been shown to be strongly associated to the mineral matrix (i.e. it is not possible to separate this OM from the minerals without harsh chemical treatment), the remaining 10% are discrete organic debris. The association between OM and the mineral matrix is thought to take place as a result of adsorption of OM to minerals prior to deposition on the seafloor and/or during the early phases of burial in the sediment. The loading of OM onto sediment particles

(expressed in $\text{mg OC} \cdot \text{m}^{-2}$) has been found to be approximately equivalent to a monolayer of proteinaceous material onto a clay particle, $0.5\text{-}1.0 \text{ mg OC} \cdot \text{m}^{-2}$ (Mayer *et al.*, 1985). Though this monolayer equivalent carbon loading is found to be nearly constant and universal in continental margin sediments, it has since been shown through TEM analysis that sediment OM is not uniformly distributed over mineral particles but forms “discrete, discontinuous blobs” on clay particles, an association primarily controlled by mineral site surface chemistry (Ransom *et al.*, 1997). In fact, only about 15% of the specific surface area of sediment particles is coated with OM (Mayer, 1999).

Mayer (1994) suggested the stability of the OM sorbed to mineral particles is related to the localization of OM within mesopores, pores within mineral surface that are $<10\text{nm}$ in width. The small size of the mesopores would render any OM localized within to become inaccessible to enzymatic attack by bacteria during transit through the water column and burial. Furthermore, the OM not localized within the mesopores but simply adsorbed to minerals may still be inaccessible to enzymatic attack due in part to steric hinderance. The close association of the OM with the mineral would create a bond with strength comparable to those of a covalent bond (Hedges & Keil, 1995).

1.3.2 Encapsulation into the mineral matrix

Sediment minerals can also physically protect OM from degradation by encapsulating molecules into the sediment matrix and preventing its chemical and enzymatic attack. The silicate sheet inter-layers of expandable clays (e.g. smectites) have been shown to shield a great deal of OM from destruction; even the application of a chemical oxidant like hydrogen peroxide was shown to be nearly ineffective (Kennedy &

Wagner, 2011). Organic matter can also be locked away by biogenic diatom frustules (composed mainly of calcium carbonate) which can shelter OM for centuries to millennia (Arnarson & Keil, 2007).

Recent studies by Lalonde et al. (2012) have suggested that reactive iron species play a role in OM preservation. Lalonde et al. (2012) propose that Fe(III) forms co-precipitates with organic matter in sediments due to the high affinity of Fe(III) for natural OM. These Fe-OM clusters would have increased stability over natural OM due to the strong Fe-OM bonds which prevent OM degradation.

1.3.3 Geopolymerization

It has been suggested that high molecular weight recalcitrant molecules can be generated *in-situ* from condensation reactions or geopolymerization of smaller, more labile molecules. For example, the formation of melanoidins can occur from the condensation of amino acids and sugars through the Maillard reaction (Maillard & Acad, 1912). There is unfortunately little direct evidence that these geopolymerization reactions actually occur; under normal conditions, abiotic condensation reactions are quite slow relative to biological uptake or remineralization (Burdige, 2006).

1.4 Non-hydrolyzable organic matter

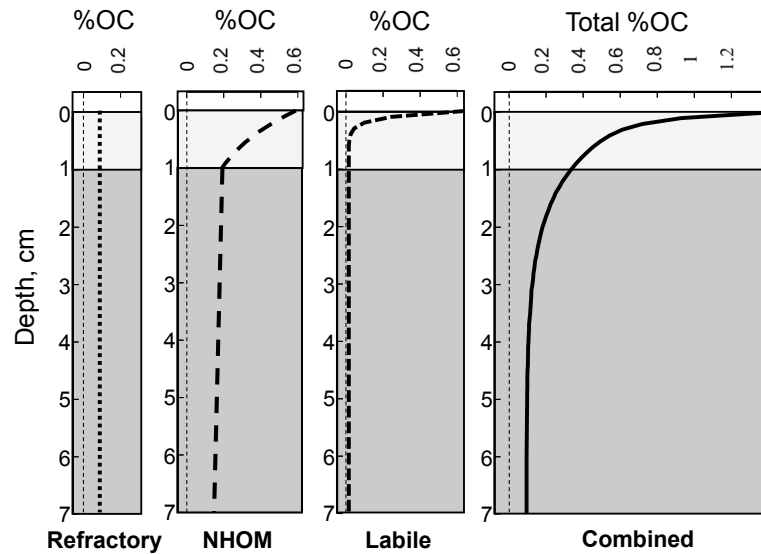
Based on its propensity towards oxidation, Hedges and Keil (1995) divided sedimentary OM into three pools: (i) totally refractory fraction, (ii) non-hydrolyzable OM that degrades only in the presence of O₂ and (iii) labile OM that degrades regardless of sedimentary redox conditions (Figure 1.2). Living organisms are almost entirely

composed of labile OM (such as proteins and carbohydrates) which degrade readily under any redox condition (Cowie & Hedges, 1992). Only a small percentage of sedimentary OM is completely insensitive to oxygen; OM which was buried for nearly 10 000 years in anoxic conditions is nearly completely remineralized (85%) when re-exposed to oxygen (Cowie & Hedges, 1992). The OM doesn't degrade unless O₂-requiring enzymes (including (i) oxidase which catalyses the transfer of an electron to O₂, (ii) dehydrogenase which removes a hydrogen, and (iii) mono/di-oxygenase which inserts O₂ into organic compounds (Sawyer, 1991)) are present that are of particular interest in the global OC cycle and budget. These O₂-sensitive, recalcitrant organic molecules tend to be oxygen poor, insoluble, highly aliphatic in nature and hydrolysis-resistant. Because of these characteristics (resistance to hydrolysis and insolubility), this portion of sediment OM can be chemically isolated from the rest of the sediment OM.

Living organisms can produce insoluble, non-hydrolyzable macromolecules that are resistant to bacterial degradation. These freshly synthesized molecules include lignin (structural biopolymer from vascular plants) and algaenans (multi-laminar cell wall component of microalgae) (Derenne *et al.*, 1992; Nip *et al.*, 1986; Tegelaar *et al.*, 1989b; Tegelaar *et al.*, 1989c; Tegelaar *et al.*, 1989a). These molecules can be selectively preserved and become enriched in the sediment compared to other types of OM (Vandenbroucke & Largeau, 2007) as shown during a chemical study of lacustrine kerogen and algaenan isolated from *Botryococcus braunii* (Largeau *et al.*, 1984).

Another possible pathway from which recalcitrant molecules can be formed is through *in-situ* formation in the sediment via random re-polymerizations (as mentioned in 1.3.3) of more labile molecules and products from the partial degradation of OM

(Vandenbroucke & Largeau, 2007). Random re-polymerizations include the (i) Maillard reaction and (ii) abiotic condensation of phenol-degradation products to yield humics (Kononova, 1966).



(from Hedges and Keil, 1995)

Figure 1.2 %OC profiles obtained through theoretical modeling of diagenesis of different reactivity classes based on their exposure to oxygen (light grey region) generating the combine graph on the right

1.5 Arrangement of thesis

The bulk of this thesis is presented in two manuscripts which will be submitted to peer reviewed journals. It is important to note that the two manuscripts have not yet been submitted for publication. They are currently being finalized and will be published shortly. All chapters are formatted in the same manner with tables and figures numbered in reference to the chapter. Chapter III follows naturally from Chapter II, therefore, the link between the two chapters will be evident in Chapter III.

Chapter II ("Bulk and spectroscopic analysis of reactivity classes of sedimentary organic matter along a freshwater – seawater transition zone") describes the implementation of a wet chemical fractionation method designed to isolate different fractions of OM based on chemical reactivities. Bulk analysis of these fractions includes stable carbon and nitrogen isotope analysis as well as elemental analysis. Spectroscopic comparisons of the non-hydrolyzable residue are made across sampling sites. Chapter III ("Molecular and spectroscopic analysis of non-hydrolyzable sedimentary organic matter from a freshwater – seawater transition zone") describes the molecular and isotopic results following the chemical oxidation of the non-hydrolyzable residue isolated in Chapter II. Additional spectroscopic results (HR MAS-NMR) will be presented in this chapter.

Contributions from other authors need to be addressed. In Chapter II, Karine Lalonde, a current Ph.D. student at Concordia University, contributed to the interpretation of the isotopic results and to the shaping of the discussion of in Sections 2.3.1 & 2 3.2. Dr. John I. Hedges (*deceased*) developed the fractionation method utilized in Chapter II however this work presents its first implementation.

In Chapter III, Dr. André Simpson, a professor at the University of Toronto, provided training for the collection of NMR spectra and contributed to the writing of the methods and interpretation of spectroscopic measurements (Sections 3.3.3 through 3.3.5 and 3.4.2)

Chapter II

Bulk and spectroscopic analysis of reactivity classes of sedimentary organic matter along a freshwater – seawater transition zone

Mina Ibrahim¹, Karine Lalonde¹, John Hedges^{2*} and Yves Gélinas¹

¹GEOTOP and Department of Chemistry and Biochemistry, Concordia University, 7141 Sherbrooke Street West, Montréal (QC), Canada, H4B-1R6

²School of Oceanography, University of Washington, Seattle WA 98195, USA

*Deceased

Corresponding author:

Yves Gélinas
Department of Chemistry and Biochemistry
Concordia University
7141 Sherbrooke Street West
Montréal (QC), Canada, H4B-1R6
Tel.: 514-848-2424 (3337)
Fax: 514-848-2868
Email: ygelinas@alcor.concordia.ca

Abstract

Marine sediments constitute the major long-term sink for organic matter (OM) on Earth (Hedges & Keil, 1995). Burial of OM plays an important role in the global cycles of carbon (C) and oxygen (O), making the elucidation of the mechanisms responsible for carbon preservation in sediments very important. We used a chemical fractionation scheme to isolate the three major sedimentary organic matter (OM) fractions based on their contrasting chemical reactivity in samples collected along a terrestrial-to-marine transition zone in southern Quebec (Canada). Following separation of the reactivity classes, bulk elemental (C and N), isotopic ($\delta^{13}\text{C}$ and $\delta^{15}\text{N}$), and spectroscopic (FTIR) analysis was used to apportion OM into the three major reactivity classes. For bulk sediments with different starting organic C and total N contents (1.36-2.01% and 0.14-0.22% respectively), the organic solvent soluble fraction accounted for between 1.3 and 10.3% of total organic C, while the acid soluble + hydrolyzable and the non-hydrolyzable + refractory components accounted for 35.7-67.5% and 23.9-54.0%, respectively. Parallel seaward enrichment in the $\delta^{13}\text{C}$ and $\delta^{15}\text{N}$ signatures of the different reactivity classes were measured along the transition zone. Spectroscopic analysis by FTIR suggests that the non-hydrolyzable fraction has a common chemical composition in both terrestrial and marine environments, with predominantly ether, carboxylic, aliphatic and aromatic moieties.

Keywords: Organic matter, sediments, preservation, non-hydrolyzable, stable isotopes, $\delta^{13}\text{C}$, $\delta^{15}\text{N}$, FTIR spectroscopy

Introduction

Marine sediments are the major terminal sink for marine and terrestrial organic matter (OM) on Earth and therefore play a central role in the cycles of carbon and oxygen (Hedges & Keil, 1995). Terrestrial OM is transported to marine systems by rivers and is ultimately buried within coastal sediments. Isotopic and molecular proxies suggest that only 1% of terrigenous OM survives the extensive bacterial and photo-chemical degradation occurring within the watershed (Hedges *et al.*, 1994). Sequestration of this small fraction of preserved OM is a vital step in the maintenance of atmospheric CO₂ and O₂ concentrations; further studies of OM preservation and degradation pathways in coastal environments are therefore warranted.

Several studies have shown that OM preservation is linked not only to its chemical structure but also to its physical form and depositional environment (Burdige, 2006, and references within). Hedges and Keil (1995) proposed that OM preservation is the result of three co-occurring and interconnected physical and chemical processes; *i*) physical protection through sorption or encapsulation within a detrital/biogenic mineral matrix, *ii*) recalcitrance of certain organic compounds that makes them naturally resistant to degradation, and *iii*) degree of exposure of OM to oxidants during their transit from the river mouth to diagenetically stable sediment layers.

The physical protection hypothesis was first formulated by Mayer (1994) as well as Keil and Hedges (1994). Because the loading of organic carbon (OC) per square meter of mineral surface is nearly constant (0.5-1.0 mg OC/m²) for coastal sediments collected around the world, it was proposed that mineral surfaces have a preservative and sheltering effect for OM. Since a large fraction of the OM is found within small pores on

the surface of minerals as well as between silicate sheets (Luthy *et al.*, 1997; Mayer *et al.*, 2004), both biological and chemical remineralization could be hampered mainly through poor accessibility and steric hindrance. Lalonde *et al.* (2012) have also shown in a recent study that a significant fraction of sedimentary OM is protected from degradation through its close association with iron oxides, mostly through direct complexation reactions and/or encapsulation.

The chemical structure of the OM also plays an important role in its resistance to remineralization. Whereas common biochemicals such as peptides, polysaccharides and simple lipids are labile under most sediment accumulating conditions, some chemical groups, such as fused aromatic rings and highly cross-linked aliphatic chains, are intrinsically recalcitrant. These recalcitrant groups are abundant in notoriously resistant molecules such as black carbon, polycyclic hydrocarbons or algeanans (Gélinas *et al.*, 2001a; Nguyen *et al.*, 2003). As degradation and reworking of sedimentary OM takes place during early diagenesis, these recalcitrant molecules account for an increasingly large proportion of bulk OM, along with bacterial cell remains that progressively replace a fraction of labile OM during early diagenesis (Tremblay & Benner, 2006). These remains are not necessarily refractory but they are continuously utilized or recycled by other bacteria.

The cumulative exposure of sediment to oxic conditions during deposition and accumulation is detrimental to OM preservation, with burial efficiency and OM composition directly influenced. (Cowie *et al.*, 1995; Gélinas *et al.*, 2001a; Hartnett *et al.*, 1998). Certain macromolecules such as lignin, cutin, hydrocarbons and algaenans, are mineralized at a much higher rate in oxic conditions (Hedges & Oades, 1997), and hence

they are selectively preserved during anoxic diagenesis. Higher sedimentation and burial rates reduces the time OM is exposed to oxic conditions and thus increases its preservation (Hedges & Keil, 1995).

Organic matter preservation in marine sediments therefore results from a dynamic balance between the protective association between OM and minerals or metal ions, and the cumulative exposure time of OM to oxic conditions. In 1995, Hedges and Keil defined three operationally defined sedimentary OM components and proposed that the relative proportions of each component in a given sample played a major role in the preservation of the bulk OM pool because of their contrasting reactivity in oxic and/or anoxic settings. The first component was defined as the labile OM fraction, generally composed of simple biochemicals which are degraded at a similar rate in both under oxic and anoxic conditions. At the other end of the spectrum is the low abundance refractory fraction, composed of recalcitrant and generally macromolecular compounds which are well preserved under both oxic and anoxic conditions. The third component is composed of non-hydrolyzable compounds, which are degraded mostly under oxic conditions. As most of the labile fraction is degraded in the water column or during the early phases of sediment diagenesis, it is the abundance of the refractory and non-hydrolyzable components and thus the cumulative exposure time to oxic conditions that ultimately controls OM preservation in sediments. Studies using $\delta^{13}\text{C}$ signatures (Hwang & Druffel, 2003) and solid-state ^{13}C NMR spectroscopy (Gélinas *et al.*, 2001b; Hwang *et al.*, 2006) have shown that the non-hydrolyzable OM fraction is likely derived from lipid-like material and is composed mostly of aliphatic and aromatic chemical groups. In transition environments such as estuaries and river deltas, it is not clear what proportion of non-

hydrolyzable OM derives from terrestrial or marine sources, and how efficiently these two non-hydrolyzable OM pools are buried and preserved.

To answer this question, we used a wet chemical oxidation scheme initially proposed by Hedges (*pers. comm.*) to fractionate OM from a series of sediments collected along a freshwater-marine transition zone (St. Lawrence Estuary, Canada) into the three broad chemical reactivity classes: (i) the solvent soluble fraction, which includes all compounds that are solubilized with a mixture of non-polar solvents (also called the 'lipid' fraction); (ii) the labile fraction, comprising acid soluble OM lost during demineralization, as well as hydrolyzable OM removed by chemical acid hydrolysis; and (iii) the non-hydrolyzable fraction that corresponds to solid phase OM remaining following demineralization and hydrolysis, including the refractory OM. Elemental (carbon and nitrogen) mass and isotopic balances were calculated, and spectroscopic characterization of the non-hydrolyzable/refractory OM fraction was done by FTIR.

Methods

2.3.1 Sampling sites

The samples were collected in Lake Jean, a typical freshwater lake from the Canadian boreal forest, and along the freshwater – salty water transition zone of the St. Lawrence Estuary (SLE) and Gulf on the northeastern North American coast (Table 2.1). The SLE system is characterized by estuarine circulation with freshwater supplied by the St. Lawrence River gradually mixing with salty water originating from the North Atlantic Ocean and the Labrador Sea (El-Sabh & Silverberg, 1990). The SLE is characterized by perennially hypoxic conditions at depth (about 55-60 μM dissolved O_2 , Gilbert et al.,

2005), owing partly to anthropogenic pressure since the start of the century but also to variations in the proportion of cold water from the Labrador Sea and warmer water from the deep Atlantic entering the St. Lawrence Trough at depth. The sampling locations either represent end-members for terrestrial (lacustrine: Lac Jean, and fluvial: Station D-E) and marine (Station 16) organic matter end-members, or a mixing zone with major contributions from the two sources (Station 23).

Table 2.1: Sample location and characteristics

| Station | Latitude (N) | Longitude (W) | Sediment Depth (cm) | Water Column Depth (m) | Bottom Water Salinity (PSU) |
|----------|--------------|---------------|----------------------------|------------------------|-----------------------------|
| Lac Jean | 46°21'43.8" | 76°20'42.0" | 0-3; 9-15 | 30 | ~0.00 |
| D-E | 47°10'49.2" | 70°37'12.6" | 0-5 | 23 | 0.095 |
| 23 | 48°42'02.4" | 68°39'03.0" | 0-5; 5-10; 15-18; 28-33 | 330 | 34.335 |
| 16 | 48°23'57.6" | 60°44'03.0" | 0-5; 10-14 | 416 | 34.832 |

2.3.2 Sampling

The samples were collected in June 2006 during a mission on the *R/V Coriolis II* using a grab (Station D-E) or boxcore sampler (Stations 23 and 16). The boxcores were sub-sampled using push cores and sliced at different depth intervals. The resulting 1- to 3-cm slices were centrifuged to remove porewaters and stored at -80°C until transported to the laboratory where they were lyophilized and homogenized. The lake sediment was

collected in June 2007 using a push core inserted by a diver. The core was treated in the same way as for the SLE samples. Several depth intervals (Station D-E: 0-5 cm; Station 23: 0-5 cm, 5-10 cm, 15-18 cm, 28-33 cm; Station 16 0-5 cm, 10-14 cm; Lac Jean 0-3 cm, 9-15 cm) were chosen for each station to probe for changes in the relative abundance of the different reactivity classes upon burial in the sediment.

2.3.3 Fractionation method

Sedimentary OM is composed of many classes of compounds that can be separated based on their chemical reactivities (Hwang *et al.*, 2006). We isolated 4 fractions (Figure 2.1) to assess their relative contribution along a continental – marine transition zone: (i) an organic solvent soluble fraction comprising mostly lipids; (ii) an acid soluble fraction consisting of organic compounds solubilized during demineralization; (iii) a hydrolyzable OM fraction corresponding mostly to polysaccharides and peptides/proteins; and (iv) a non-hydrolyzable fraction that includes the quantitatively less important refractory OM fraction.

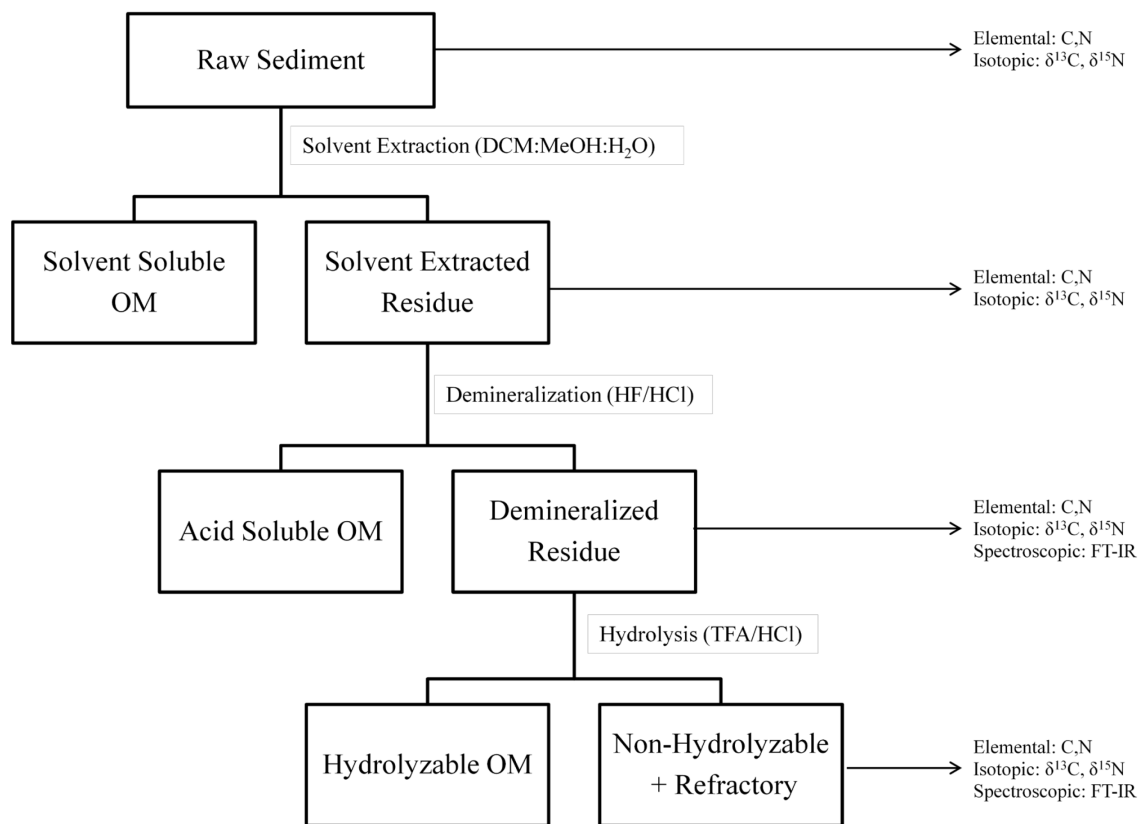


Figure 2.1 Schematic of the wet chemical fractionation method used to isolate the different reactivity classes

2.3.3.1 Solvent extraction

Dried sediments from the SLE (50 g) and Lake Jean (15 g), corresponding to approximately 1 g of organic carbon (OC), were extracted with a 3:2:1 mixture of dichloromethane:methanol:water. The samples were sonicated (Branson® 5210 Ultrasonic bath) for 10 minutes and shaken overnight. They were then centrifuged at 3000 g for ten minutes and the supernatants were collected with a combusted glass pipet. These steps were repeated 10 times to ensure maximum extraction of the solvent soluble compounds. Upon completion of the extraction, the samples were freeze-dried, weighed and sub-sampled for elemental analysis. The supernatants were dried by rotary

evaporation and analyzed by EA-IRMS to estimate the percentage of OC removed and the $\delta^{13}\text{C}$ isotopic signature of this fraction.

2.3.3.2 Demineralization

Dried residues from the previous step were first treated with 24 ml of 1N hydrochloric acid (HCl) and shaken for 1 hour to remove carbonates. The samples were then centrifuged and the supernatant discarded. A 10% hydrofluoric acid (HF) and 1N HCl solutions (25 ml) were then added to the wet samples. The samples were shaken for 48 hours before centrifuging and removing the supernatant. Four more such treatments with the HF-HCl solution were completed before increasing the HF concentration to 48% and shaking for 48 hours to target the more refractory minerals. This last treatment was repeated between 3 and 5 times until the sample mass was reduced by >95%. The samples were then treated with 1.33 grams of boric acid (H_3BO_3) in 10 mL of 5% HF and shaken overnight to remove any fluoride-containing minerals (such as CaF_2 for instance) formed during demineralization. The samples were again centrifuged, the supernatants were discarded and the samples were washed 3 times with ultrapure water before freeze-drying, weighing and sub-sampling. This treatment targets minerals and acid soluble organic compounds adsorbed onto, or encapsulated within, the mineral matrix.

2.3.3.3 Hydrolysis

Dried residues from the demineralization step were treated with 10 mL of 2N trifluoroacetic acid (TFA), purged with N_2 gas and placed in an oven at 100°C for 3 hours. The samples were centrifuged and the supernatants discarded. The samples were then treated five times in the same way with 6N TFA to remove all hydrolyzable

polysaccharides. After the 5th TFA treatment, the samples were treated with 6N HCl, purged with N₂ and placed in an oven at 95°C for 24 hours to hydrolyze proteins and peptides. After cooling, the samples were centrifuged and the supernatants were discarded. The residues were then rinsed 3 times with ultrapure water. The rinsed samples were freeze-dried, weighed and sub-sampled. Following this last treatment, the OM remaining in the residue comprised non-hydrolyzable and refractory material only.

2.3.4 Elemental and isotopic analysis

The residue remaining following each treatment was analyzed for elemental and isotopic composition. The non-demineralized samples were first treated with HCl in the vapor phase to remove carbonates. Percentages of organic carbon and total nitrogen, as well as the $\delta^{13}\text{C}$ and $\delta^{15}\text{N}$ compositions, were obtained using an EuroVector 3028-HT elemental analyzer (EA), coupled to a GV Instruments (now Elementar) Isoprime isotope ratio mass spectrometer (IRMS). The EA-IRMS was calibrated for mass and isotopic composition using the laboratory standard β -alanine and pre-calibrated IAEA certified primary standards sucrose for carbon and ammonium sulfate for nitrogen. The analytical precision was ± 0.02 ‰ for ^{13}C , ± 0.05 ‰ for ^{15}N , and ± 0.2 % for C and N contents.

2.3.5 FT-IR

The chemical composition of the demineralized and demineralized/hydrolyzed residues was assessed using FTIR spectroscopy analysis. To allow direct comparison of the relative absorption band intensities, the samples were precisely mixed with potassiumbromide (KBr) salt to obtain a final concentration of 1% carbon by mass. The

KBr pellet was formed under pressure with exactly 100 mg of the KBr-sample mix and then dried overnight in a vacuum desiccator. Samples were placed in a pellet holder and analyzed with a Thermo Nicolet 6700 ® FTIR spectrometer. The chamber was purged with nitrogen gas (N₂) for 15 minutes before acquiring the spectra (64 scans at a resolution of 4 cm⁻¹).

Results and discussion

The relative contribution of the selected reactivity classes, stable carbon and nitrogen isotope abundances as well as atomic C/N ratio for the different samples and fractions are presented in Table 2.2. We have combined certain fractions owing to specificity issues associated with the method used in this work; for instance, the very long reaction time necessary to completely demineralize the samples with the HCl-HF mixture likely leads to partial hydrolysis of the more labile hydrolyzable compounds. The acid-soluble OM fraction, released during demineralization, was thus combined with the hydrolyzable OM fraction. The same is true for the non-hydrolyzable and the refractory OM fractions that cannot be quantitatively separated using this method. The isolated fractions were operationally defined and roughly correspond to broad classes of biochemicals: lipid-like hydrophobic compounds for organic solvent soluble fraction, small hydrophilic molecules for the acid-soluble fraction, peptides, proteins and carbohydrates for hydrolyzable OM, high molecular weight, cross-linked aromatic, phenolic or aliphatic compounds for the non-hydrolyzable fraction and condensed graphitic polyaromatic compounds (Dickens *et al.*, 2004) for the refractory fraction.

Note that the demineralization method was designed to avoid the formation of melanoidin, a recalcitrant product formed from the condensation of peptides and sugars at high temperatures (Maillard & Acad, 1912), which would lead to an overestimation of the non-hydrolyzable + refractory fraction at the expense of the acid soluble + hydrolyzable fraction. This was done by sequentially hydrolyzing polysaccharides with a non-oxidizing acid (trifluoroacetic acid) and peptides with HCl (Allard *et al.*, 1998). In addition, previous studies have shown that the HF + HCl mixture used to demineralize

the samples has minimal effect on the chemical composition of hydrolyzable and non-hydrolyzable OM, and thus we assume that any minor compositional change has not affected the chemical reactivity of the different OM fractions (Eusterhues *et al.*, 2007; Gélinas *et al.*, 2001b; Rumpel *et al.*, 2006).

Elemental concentrations and stable isotope signatures of carbon and nitrogen have been used extensively to determine the sources and diagenetic state of sedimentary OM in coastal systems (Orginc *et al.*, 2005). Stable carbon isotope signatures can be used to assess OM sources, while stable nitrogen isotope signatures have been shown to reflect nutrient usage/cycling and trophic level (Altabet & Francois, 1994). Early diagenesis however, can blur the interpretations that are drawn from the stable isotope abundances. In particular, selective preservation of specific organic compounds with distinct signatures or isotopic fractionation caused by enzymatic OM processing can exert a strong influence on the $\delta^{13}\text{C}$ and $\delta^{15}\text{N}$ signatures found in complex samples such as sedimentary OM (Prahl *et al.*, 1997). These processes particularly limit the usefulness of nitrogen isotopes for determining source of the OM. Care must therefore be taken when interpreting the isotopic signal measured for sedimentary OM; however, these diagenetic processes have a less severe impact in coastal transition zones such as estuaries and river deltas where large isotopic differences exist between terrestrial and marine compounds (Hayes, 1993).

2.4.1. Elemental composition

The OC and TN concentrations were high in Lake Jean (about 12% and 1%, respectively), reflecting lower dilution of the sedimentary OM pool by minerals compared to fluvial and estuarine environments. The OC concentrations varied little

along the SLE transect, with concentrations ranging from 1.3 to 2.0 %, while TN concentrations increased offshore relative to OC (Table 2.2). As a result, atomic C/N ratios decreased from 16.7 at station DE, reflecting a higher proportion of OM derived from vascular plants, to 8.36 at station 16 where inputs were predominantly derived from N-rich marine OM. The C/N ratios increased down core at Station 23 from a value of 10.3 +/-0.02 to 12.3 +/-0.02, suggesting a preferential degradation and removal of N-rich compounds (Peters *et al.*, 1978).

The relative abundances of the main fractions isolated in this work varied between samples (Figure 2.2). The organic solvent soluble, or lipid fraction was the least abundant in all samples and accounted for between 2 and 10% of total OC at all sampling sites (Figure 2.2a). Surprisingly, lipids were generally more abundant at Station 23 compared to the other stations. Using amino acid and chlorin degradation indexes, Alkhatib *et al.* (2012) found less degraded OM at this station compared to Stations DE and 20, and attributed this relative freshness to the lower levels of dissolved oxygen in the bottom waters, and thus lower oxygen exposure times, at this station.

The acid-soluble + hydrolyzable fraction made up the largest proportion of total OC at all sampling sites (49 +/-0.1 to 69 +/-0.14 % of total OC), except for the most down core sample at Station 23. The relative abundance of this fraction generally decreased seaward and down core, in agreement with the more degraded state of OM reported in these samples (Alkhatib *et al.*, 2012). The relative abundance of the non-hydrolyzable + refractory fraction followed an opposite trend, with higher values at Station 16 and down core compared to the more terrestrial or surface samples.

The TN distribution among the different fractions was much less variable; between 80 ± 0.16 and $93 \pm 0.19\%$ of TN was recovered in the acid soluble and hydrolyzable fractions, while the rest was found in the non-hydrolyzable + refractory fraction (Figure 2.2b). The very high proportion of TN found in the hydrolyzable fraction suggests that most sedimentary nitrogen is derived from hydrolyzable compounds such as proteins, peptides and aminosugars, with possibly small contributions from pigments and nucleic acids. There was no clear trend in the data, except for slightly higher relative contributions to TN for the non-hydrolyzable and refractory fraction in the deep sediment layer in Lake Jean and at Station 16.

Contrasting atomic C/N ratios were measured for the different fractions of each sediment sample, particularly for the more terrestrially influenced samples (Figure 2.2c). While the acid soluble + hydrolyzable fractions were generally enriched in nitrogen relative to the bulk sample (low C/N ratios varying between 5.8 ± 0.01 and 13.4 ± 0.02), the ratios measured for the non-hydrolyzable + refractory fractions were above 40 for Lake Jean and Station DE sediments (two mostly terrestrial sites), and at Station 23 below 15cm, and between 15.9 and 29.6 for the more marine samples (shallow sediment layers at Station 23 and both Station 16 samples). Based on sedimentation rates reported by Smith and Schafer (1999), the two deep samples at Station 23 correspond to the height of the pulp and paper contamination in the St. Lawrence River watershed (15-18 cm, 1973-1978), and to pre-industrial conditions when coastal eutrophication was not an issue (28-33 cm 1944-1954).

2.4.2. Isotopic composition

Several trends emerged from the analysis of the $\delta^{13}\text{C}$ signatures (Figure 2.2d). The organic solvent soluble fraction always had very depleted isotopic composition, while the hydrolyzable fraction was the most enriched. The non-hydrolyzable + refractory fraction was also depleted relative to the bulk sample and the acid soluble + hydrolyzable OM, which agrees with the hypothesis of lipid-like compounds being major contributors to the non-hydrolyzable fraction (Hwang & Druffel, 2003). Down core lipid and non-hydrolyzable + refractory fractions were also slightly depleted compared to surface ones, which again suggests that the most refractory compounds generally bear a more depleted $\delta^{13}\text{C}$ signature.

The most striking feature however is the general seaward trend towards more enriched $\delta^{13}\text{C}$ signatures for all fractions. This trend implies that the differences in isotopic composition of individual biochemicals is not an intrinsic characteristic of the compounds but rather reflect the source of carbon used as a building block (e.g., atmospheric CO_2 or dissolved HCO_3^- for primary producers) and the enzymatic fractionation associated with the synthesis of the compounds. The integrated origin of the OM (terrestrial or marine) is thus the main driver for the isotopic composition of bulk sediments rather than variations in the relative proportions of biochemicals with contrasting intrinsic $\delta^{13}\text{C}$ signatures. While variations in the relative proportions of the different classes of biochemicals found in a sample can lead to significant variations of the bulk $\delta^{13}\text{C}$ signature (as seen down core in our samples for example), differences in the relative proportions of marine and continental OM sources cause more significant $\delta^{13}\text{C}$ variation in most coastal settings. However, even though bulk sediment $\delta^{13}\text{C}$

signatures are very useful for determining the relative proportions of terrestrial and marine OM in a sample, an approach that targets the $\delta^{13}\text{C}$ signatures of specific fractions of OM, or even single compounds (compound-specific stable isotope analysis), may yield a clearer image of the relative proportion of each source of OM.

Nitrogen stable isotope abundances followed the opposite trend with a general enrichment of the acid-soluble + hydrolyzable fraction seaward (Figure 2.2e). The $\delta^{15}\text{N}$ signatures in this system are mostly influenced by the proportion of the two major sources, vascular plants and plankton (0.4‰ and 8.6‰, respectively; Peterson *et al.*, 1978). Noteworthy, the $\delta^{15}\text{N}$ signature of the non-hydrolyzable + refractory fraction does not vary much between samples, except for a slight enrichment at Station 16. This result suggests that both terrestrial and marine organisms produce N-containing non-hydrolyzable material, in agreement with the higher proportion of TN found in this fraction at Station 16 compared to the other stations (Figure 2.2b).

Table 2.2. Organic carbon (OC) and total nitrogen (TN) contributions of the different OM fractions to total organic matter, and their elemental and isotopic signatures. The analytical precision was ± 0.02 ‰ for ^{13}C , ± 0.05 ‰ for ^{15}N , and ± 0.2 % for C and N contents

| Station (depth) | Org. Matter Fraction | Org. Carbon (% of total) | Tot. Nitrogen (% of total) | (C/N) _a ratio | $\delta^{13}\text{C}$ (‰) | $\delta^{15}\text{N}$ (‰) |
|-----------------------|----------------------|--------------------------|----------------------------|--------------------------|---------------------------|---------------------------|
| Lac Jean (0-3 cm) | Untreated | 12.44* | 1.00* | 14.49 | -26.49 | 2.35 |
| | Lipids | 3.02 | n.a. | n.a. | -36.60 | n.a. |
| | Ac sol. + hydrol. | 67.46 | 93.91 | 13.41 | -25.99 | 3.01 |
| | NHOM + refractory | 29.52 | 6.09 | 33.83 | -26.93 | 1.38 |
| Lac Jean (9-15 cm) | Untreated | 12.21* | 1.02* | 14.11 | -27.08 | 2.69 |
| | Lipids | 1.79 | n.a. | n.a. | -66.21 | n.a. |
| | Ac sol. + hydrol. | 55.42 | 85.39 | 10.27 | -25.35 | 3.42 |
| | NHOM + refractory | 42.79 | 14.61 | 31.33 | -27.70 | 2.36 |
| Station D-E (0-5 cm) | Untreated | 2.01* | 0.14* | 16.74 | -25.93 | 3.82 |
| | Lipids | 4.23 | n.a. | n.a. | -35.47 | n.a. |
| | Ac sol. + hydrol. | 66.82 | 92.05 | 10.35 | -24.79 | 3.76 |
| | NHOM + refractory | 28.95 | 7.95 | 36.26 | -27.09 | 2.33 |
| Station 23 (0-5 cm) | Untreated | 1.36* | 0.15* | 11.95 | -23.91 | 5.86 |
| | Lipids | 8.26 | n.a. | n.a. | -25.76 | n.a. |
| | Ac sol. + hydrol. | 62.08 | 86.89 | 7.80 | -22.83 | 6.03 |
| | NHOM + refractory | 29.66 | 13.11 | 25.33 | -25.64 | 2.33 |
| Station 23 (5-10 cm) | Untreated | 1.51* | 0.16* | 13.75 | -24.15 | 3.91 |
| | Lipids | 8.28 | n.a. | n.a. | -27.75 | n.a. |
| | Ac sol. + hydrol. | 67.86 | 89.36 | 9.10 | -23.40 | 6.28 |
| | NHOM + refractory | 23.86 | 10.64 | 18.92 | -25.85 | 2.91 |
| Station 23 (15-18 cm) | Untreated | 1.32* | 0.13* | 13.09 | -24.33 | 4.63 |
| | Lipids | 2.32 | n.a. | n.a. | -35.16 | n.a. |
| | Ac sol. + hydrol. | 57.75 | 91.08 | 8.07 | -23.23 | 6.07 |
| | NHOM + refractory | 39.92 | 8.92 | 32.54 | -25.95 | 2.63 |
| Station 23 (28-33 cm) | Untreated | 1.29* | 0.12* | 12.60 | -24.25 | 4.81 |
| | Lipids | 10.31 | n.a. | n.a. | -25.92 | n.a. |
| | Ac sol. + hydrol. | 35.68 | 88.94 | 5.83 | -21.67 | 5.59 |
| | NHOM + refractory | 54.01 | 11.06 | 34.54 | -26.30 | 2.19 |
| Station 16 (0-5 cm) | Untreated | 1.79* | 0.25* | 9.36 | -22.08 | 6.62 |
| | Lipids | 2.61 | n.a. | n.a. | -25.68 | n.a. |
| | Ac sol. + hydrol. | 51.61 | 87.25 | 7.69 | -20.73 | 6.54 |
| | NHOM + refractory | 45.77 | 12.75 | 19.12 | -23.73 | 3.98 |
| Station 16 (10-14 cm) | Untreated | 1.65* | 0.22* | 8.66 | -21.91 | 6.40 |
| | Lipids | 1.27 | n.a. | n.a. | -26.32 | n.a. |
| | Ac sol. + hydrol. | 48.92 | 79.83 | 5.94 | -20.61 | 6.90 |
| | NHOM + refractory | 49.81 | 20.17 | 22.19 | -23.69 | 3.88 |

*Values are the measured % carbon and nitrogen concentrations rather than their relative contribution to total OM (% of total)

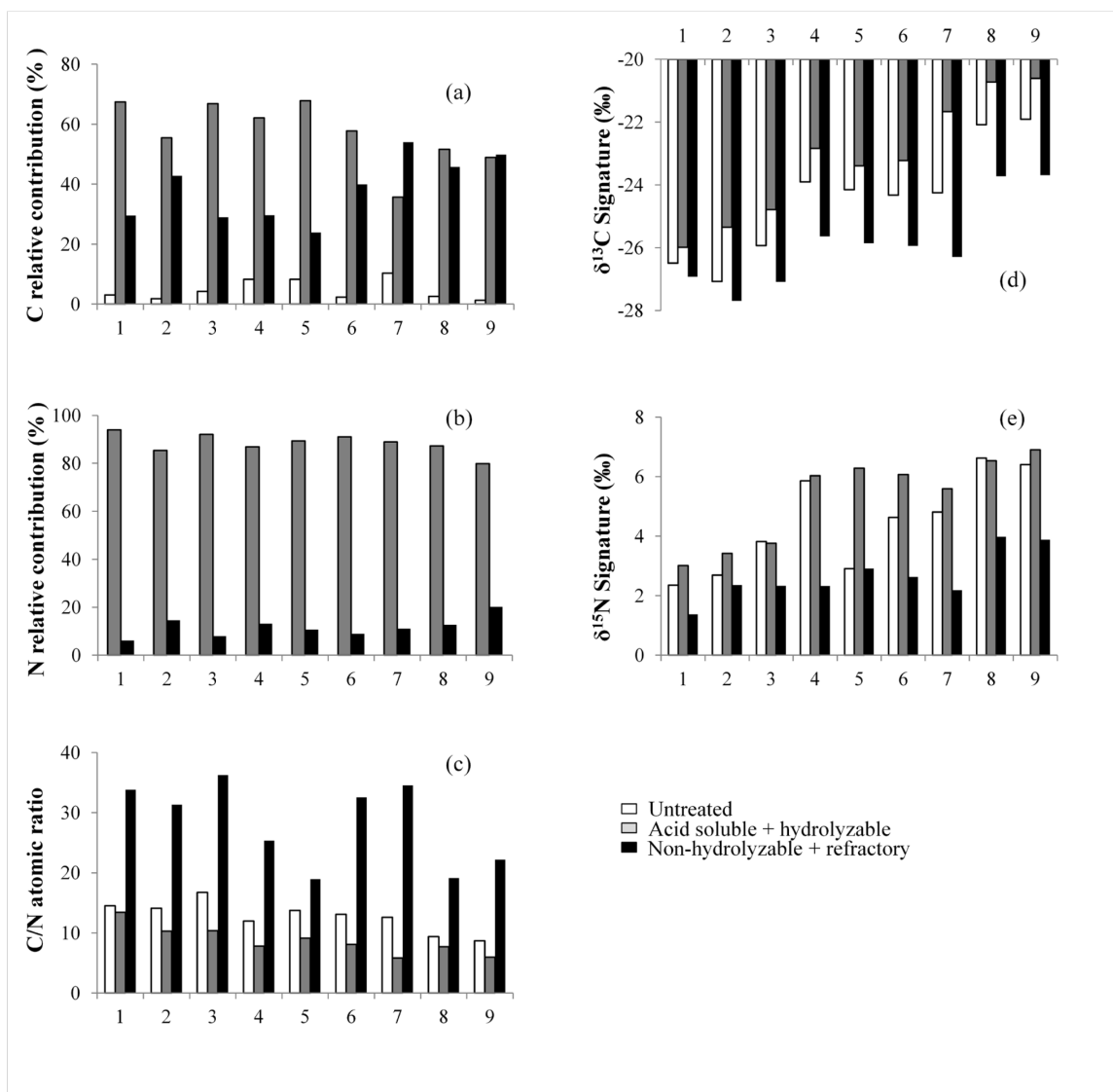


Figure 2.2 Contribution of different reactivity classes to (a) total OC, (b) total N, and their (c) C/N atomic ratios, (d) $\delta^{13}\text{C}$ and (e) $\delta^{15}\text{N}$ signatures. Sample numbers correspond to Lake Jean 0-5 cm (1) and 9-15 cm (2); Station DE (3); Station 23 0-5 cm (4) 5-10 cm (5), 15-18 cm (6), 28-33 cm (7); Station 16 0-5 cm (8) and 10-14 cm (9)

2.4.3 FT-IR

The FT-IR spectroscopic analysis was conducted on demineralized samples before and after the hydrolysis step to probe for variations in the relative abundance of the different functional groups between the two fractions. In particular, we wanted to assess whether functional groups that are specific to hydrolyzable material, such as the amide group of proteins and peptides for example, were still detectable in the non-

hydrolyzable OM fraction. To allow direct comparison of relative intensities for each functional group between spectra, the OC:KBr ratio and the total mass of KBr used to make the pellets were kept constant for each sample.

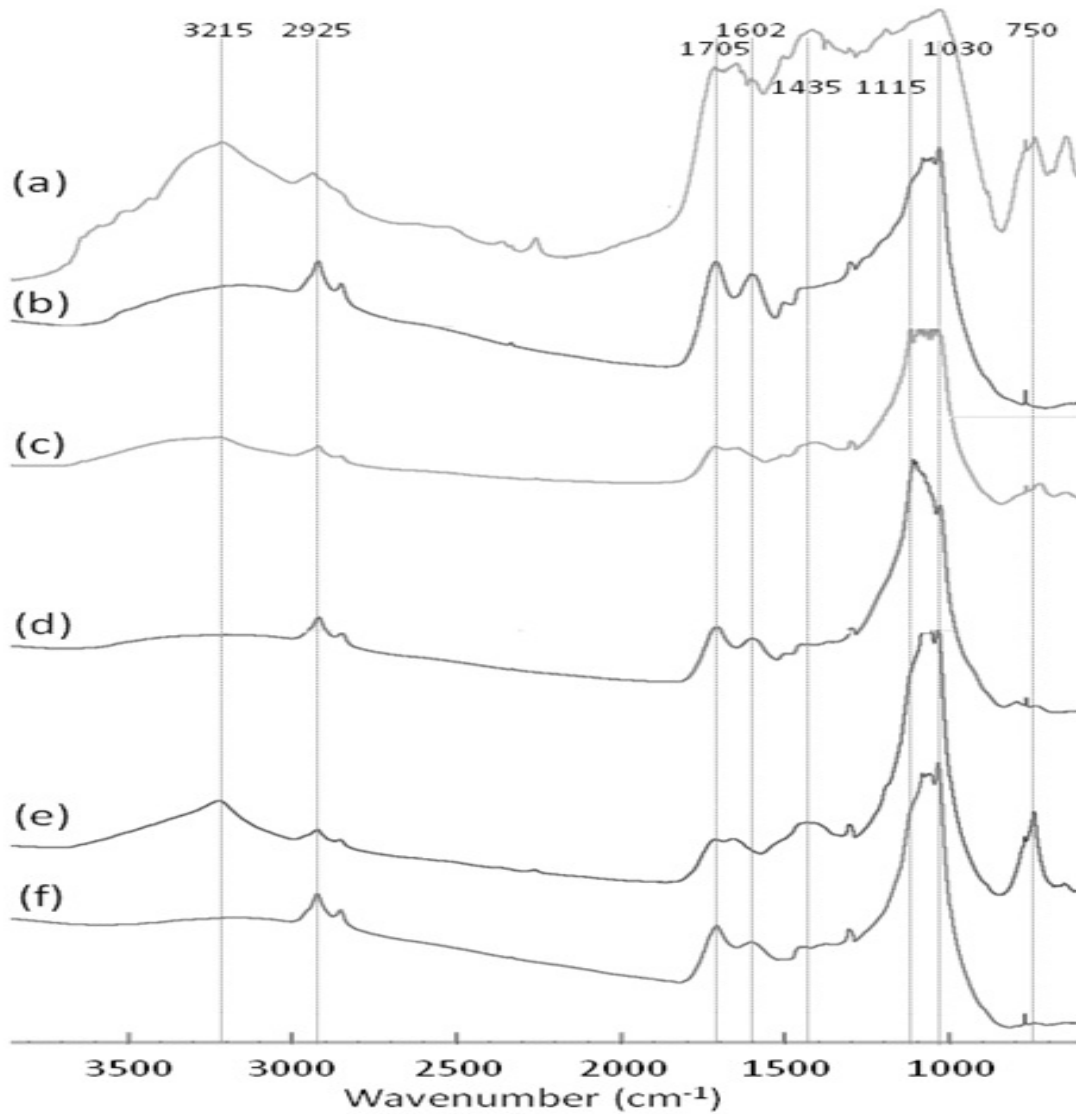


Figure 2.3 FT-IR spectra of demineralized samples of surface sediments (0-5 cm) from stations (a) D-E, (c) 23 and (e) 16, as well as for the demineralized + hydrolyzed samples from stations (b) D-E, (d) 23, and (f) 16. The numbers at the top correspond to wavenumbers of interest that are discussed in the text. Each pellet weighed 100 mg with 1% carbon content by weight.

Figures 2.3a-f show the spectra acquired for the demineralized (Figures 2.3a, 2.3c and 2.3e) and demineralized + hydrolyzed (Figures 2.3b, 2.3d and 2.3f) samples. All spectra show a broad peak between 3000 and 3700 cm^{-1} , corresponding to H-bonded OH stretching derived from a broad range of molecules, with possibly a small contribution from the N-H stretch absorption band of amines and amides. This band is sharper and more intense in the demineralized samples, peaking at 3215 cm^{-1} , most likely because of the removal of simple hydroxyl bearing molecules such as polysaccharides. On the contrary, the absorption band peaking near 2925 cm^{-1} and representing C-H stretching of methyl and aldehyde functional groups is more intense in the demineralized + hydrolyzed samples, suggesting selective preservation of aliphatic compounds upon hydrolysis. Absorption bands for C=O and C=C functionalities are intense in the 1500 to 1750 cm^{-1} region in all the demineralized samples. Their relative proportion change following hydrolysis with the band centered around 1705 cm^{-1} becoming the most abundant in this region of the spectrum. The wavenumber region between 1470 and 1380 cm^{-1} and centered around 1435 cm^{-1} is a significant contributor in all demineralized spectra and is attributed to CH_2 and CH_3 bending; surprisingly, while the bands around 2925 cm^{-1} became more intense upon hydrolysis, the abundance of the broad band peaking at 1435 cm^{-1} decreased, suggesting that the two functionalities were part of compounds belonging to different reactivity classes. The C-O stretch bands for the tertiary, secondary and primary alcohols between 1150 and 1000 cm^{-1} changed very little upon hydrolysis at stations DE and 16. Other functional groups (Si-O and S=O) are also known to absorb in the same spectral window but their contribution is assumed to be small in demineralized and demineralized + hydrolyzed samples. Although the series of peaks in the 700-1000

cm⁻¹ region of some spectra might be indicative of differences in alkene isomers and/or benzene substitution patterns, the associated alkene C–H stretch absorption normally seen at 3000-3100 cm⁻¹ is absent from all spectra most likely because of the intensity of the O–H stretch band. Contributions from different mineral species also cannot be ruled out below 1000 cm⁻¹.

The important differences that can be seen between the spectra of the demineralized and demineralized + hydrolyzed samples are mostly linked to variations in the relative contributions from the five major regions of the spectrum upon hydrolysis, namely, (i) decrease in O–H/N–H stretching band intensity between 3000 and 3700 cm⁻¹, (ii) increase in C–H stretching band intensity between 2800 and 2950 cm⁻¹; (iii) decrease in C=O and C=C stretching band intensities between 1500 and 1700 cm⁻¹, (iv) decrease in C–H bending band intensity between 1470 and 1380 cm⁻¹, and (v) small shifts in relative peak intensities within the C–O stretching region between 1170 and 1000 cm⁻¹. These regions are in large part associated with easily hydrolyzable material (proteins/peptides and polysaccharides) that are removed upon hydrolysis (Samios *et al.*, 2007).

Surprisingly, the chemical composition of residual non-hydrolyzable + refractory material is very similar in all three samples despite differences in the proportion of terrestrial and marine organic matter at each site: it is composed mostly of O–H/N–H, C–H (stretching, little bending), C=O, C=C and C–O functional groups. Such composition, along with the very intense C–O stretching band, agrees with previous papers (Blokker *et al.*, 1998; Gélinas *et al.*, 2001a; Hwang *et al.*, 2006) reporting on the chemical composition of algaenans (aliphatic-rich macrobiopolymers cross-linked through ether bonds and with varying proportions of aromatic functional groups). The fact that the

terrestrial sample showed very little compositional difference suggests that lignin-derived compounds (enriched in C=C and O-H functionalities) could be less resistant than anticipated to hydrolysis, particularly when using multiple consecutive treatments and long reaction times, such as in our method. The removal of a large fraction of the lignin (but not all) during demineralization and/or hydrolysis was confirmed using a soft oxidation method with CuO followed by gas chromatographic analysis (results to be published elsewhere).

Conclusion and implications

Our work highlighted significant trends in the relative abundances of the different OM reactivity classes in lake and estuarine sediments. We found a general seaward decrease in the abundance of the more labile soluble and hydrolyzable OM fraction, paralleled by an increase in the abundance of the more resistant non-hydrolyzable and refractory material. Such a shift is most likely caused by the fact that OM in our marine samples is more degraded than in the mixed or terrestrial samples owing to the lower sediment accumulation rates (Smith and Schafer, 1999), and the longer cumulative exposure time to oxic conditions in the water column and at the surface of the sediment (Alkhatib *et al.*, 2012). This result agrees with the hypothesis of preferential preservation of a non-hydrolyzable and refractory OM component in sediments (Gélinas *et al.*, 2001a).

The variations found in $\delta^{13}\text{C}$ signatures and in the relative abundance of the different functional groups suggest that the non-hydrolyzable and refractory component is derived mostly from non-extractable, lipid-like material enriched in C-C and C=C bonds, in agreement with the results of Hwang *et al.* (2006) for sinking particles of the Pacific Ocean. This non-hydrolyzable OM fraction is also enriched in C-O functionalities,

possibly acting as ether cross-links between lipid-derived aliphatic moieties (Blokker *et al.*, 1998). Interestingly, the chemical composition of non-hydrolyzable OM varied very little between terrestrially-dominated samples and marine samples. Although speculative and not taking into account mineral protection mechanisms such as clay mineral (Mayer, 1994) or iron oxide (Lalonde *et al.*, 2012) protection, this finding suggests (i) that the fraction of OM that is most resistant towards biological degradation in aquatic sediments, whether terrestrial or marine, is similar in composition, and (ii) on very long time scales, lignin derived compounds might not be as resistant to degradation as previously thought. This last conclusion would explain why so little lignin is found in marine sediments (Hedges *et al.*, 1997). Interestingly, despite the seemingly similar chemical composition of the non-hydrolyzable plus refractory OM fraction in terrestrial and marine samples, the $\delta^{13}\text{C}$ and $\delta^{15}\text{N}$ signatures of the non-hydrolyzable plus refractory fraction varies by more than 3‰ and 1.5‰, respectively, between Stations DE (terrestrial) and 16 (marine), indicating that both continental and marine organisms synthesize these resistant compounds (or their building blocks). Additional molecular-level oxidation studies on the macromolecular composition of the non-hydrolyzable + refractory fraction should be carried out to get a better understanding of the source and structure of this quantitatively important component of aquatic sediments.

CHAPTER III

Molecular and spectroscopic analysis of non-hydrolyzable sedimentary organic matter from a freshwater – seawater transition zone

Mina Ibrahim¹, André Simpson² and Yves Gélinas¹

¹ GEOTOP and Department of Chemistry and Biochemistry, Concordia University, 7141 Sherbrooke St. West, Montréal, QC, Canada, H4B 1R6

² Department of Chemistry, University of Toronto, Scarborough Campus, 80 St. George St., Toronto, ON, Canada, M5S 3H6

Corresponding author:

Yves Gélinas
Department of Chemistry and Biochemistry
Concordia University
7141 Sherbrooke Street West
Montréal (QC), Canada, H4B-1R6
Tel.: 514-848-2424 (3337)
Fax: 514-848-2868
Email: ygelinas@alcor.concordia.ca

Abstract

Aquatic sediments can be fractionated into a series of operationally defined components based on chemical reactivity. One of these components, the non-hydrolyzable organic matter (NHOM) fraction, is highly resistant to microbial degradation in anoxic settings (Hedges & Keil, 1995) and plays an important role in the preservation and ultimate burial of OM in sediments. Early studies have suggested that the NHOM fraction is composed primarily of algal microfossils, referred to as algaenan (Gelin *et al.*, 1997). To assess the marine contribution to the NHOM component, we characterized NHOM using NMR spectroscopy and ruthenium tetroxide (RuO₄) oxidation in a series of samples from a terrestrial to marine transition zone of southern Quebec (Canada). Solid state ¹³C, ¹H and ¹H-¹³C nuclear magnetic resonance (NMR) analyses have shown NHOM to be highly aliphatic in nature with a slight contribution from aromatic moieties, which decreases in abundance in marine samples. The relative abundances and stable carbon isotope signatures of the products generated upon RuO₄ oxidation (alkanoic and alkandioic acids) suggest that chemical composition, rather than the origin of the material (terrestrial or marine), determines the preservation and burial potential of the NHOM component.

Keywords: Organic matter, marine sediments, preservation, non-hydrolyzable organic matter, stable isotopes, $\delta^{13}\text{C}$, $\delta^{15}\text{N}$, compound-specific stable isotope analysis
NMR spectroscopy

Introduction

Sedimentary OM is a complex continuum of molecules with different chemical groups, reactivities and molecular weights. One operationally defined fraction of OM that is of interest is the non-hydrolyzable (NHOM) fraction due to its resistance to both microbial and chemical degradation under anoxic conditions (Hedges & Keil, 1995). Because normal coastal sediments are generally devoid of oxygen within a few millimeters to a few centimeters below the sediment-water interface, the NHOM fraction plays an important role in determining the OM burial efficiency in sediments. NHOM is believed to be composed of highly amorphous, insoluble, high molecular weight OM, often referred to as protokerogen. Protokerogen, and its more matured form, kerogen are derived from algal microfossils, an ultralaminar cell layer (Gelin *et al.*, 1997). This ultralaminar cell layer, while composing 1-2% of the total dry mass, becomes a major contributor to kerogen through selective preservation (Schouten *et al.*, 1998).

Previous molecular studies on the NHOM fraction have shown that these algal microfossils are mostly composed of an insoluble, aliphatic material called algaenan (Augris *et al.*, 1998; Blokker *et al.*, 1998; Gelin *et al.*, 1997; Gelin *et al.*, 1994; Hwang & Druffel, 2003). Blokker *et al.* (2000) proposed a structure for algaenan comprising mostly saturated long-chain hydrocarbons with terminal acidic groups, with ether linkages connecting the different layers. These structures are difficult to study at the molecular level given the fact that they are insoluble in organic solvents and cannot be cleaved in acidic or basic conditions.

The mild oxidative RuO₄ depolymerization treatment has previously been applied in the study of NHOM, such as kerogens (Yoshioka & Ishiwatari, 2005). RuO₄

selectively oxidizes tertiary carbons, ethers and esters into carboxylic acids. Other available oxidizing agents also cleave these chemical groups; however RuO₄ also chemoselectively targets aromatic substituents oxidizing them into their corresponding carboxylic acids. RuO₄ seems to be the most suitable agent as it has been used previously to successfully produce information on the chemical structure of algaenans (Blokker *et al.*, 1998; Blokker *et al.*, 2006; Gelin *et al.*, 1997; Schouten *et al.*, 1998). RuO₄ oxidation leads to the production of a series of carboxylic and dicarboxylic fatty acids that are amenable to gas chromatography following derivatization.

In this study, we employed both spectroscopic and molecular methods in order to further probe the chemical composition and structure of the NHOM fraction. Solid state ¹³C and high resolution ¹H NMR were applied to several samples along a freshwater – seawater transition zone in southern Quebec (Canada) to determine if there is a common chemical composition to this fraction. RuO₄ oxidation was also utilized to gain insight on the structure of the NHOM fraction, and to test whether the structure is affected by differences in the origin of the OM (terrestrial or marine). Compound-specific stable isotopic analysis ($\delta^{13}\text{C}$) of the liberated acids may also reveal clues to the origin of the NHOM fraction within the continental or marine realms.

Methods

3.3.1 Sampling

The estuarine sediments were collected in June 2006 during a sampling mission on the *R/V Coriolis II*, using a grab (Station D-E) or boxcore sampler (Stations 23 and 16). The boxcores were sub-sampled using push cores and sliced at different depth intervals. The resulting 1- to 3-cm slices were centrifuged to remove pore waters and stored at -80°C until transported back to the laboratory where they were lyophilized and homogenized. The Lake Jean sediment sample was collected in June 2007 using a push core inserted by a diver. The core was treated in the same way as for the SLE samples.

3.3.2 NHOM isolation

Bulk sediment was subjected to a sequential wet chemical fractionation in order to isolate the NHOM fraction (Chapter II). Bulk sediment, 50 g dry weight, was repeatedly extracted with a mixture of 30 ml of dichloromethane, methanol and water (DCM:MeOH:H₂O) in a 3:2:1 volume ratio in order to remove lipid-like solvent soluble OM. The residue was then demineralized in a mixture of 25 ml of 10% hydrofluoric acid (HF) and 1N hydrochloric acid (HCl) to remove carbonate and clay minerals, as well as hard oxides. This procedure was repeated until the mass of the residue was reduced by more than 95%. The residue was then treated with a solution containing 1.33 grams of H₃BO₃ in 10 mL of 5% HF which dissolved any fluoride-containing minerals that may have formed during demineralization. The remaining residue was then hydrolyzed using trifluoroacetic acid (polysaccharides) and HCl (proteins and peptides) to remove hydrolyzable OM, which has a much lower potential for long-term preservation in marine

sediments compared to non-hydrolyzable and refractory material. The hydrolyzed residue was rinsed 3 times with deionized water then freeze-dried, analyzed for organic carbon and total nitrogen, and used as is for the spectroscopic and molecular-level studies described below. Note that this fraction also comprised a minor refractory OM component which differs from NHOM by the fact that it is equally resistant to degradation under both oxic and anoxic conditions (while NHOM is not resistant to long-term degradation under oxic conditions). The refractory component, composed mostly of condensed polyaromatic compounds, is however much less abundant than the NHOM component.

3.3.3 ^{13}C Solid-state NMR spectroscopy

For solid state ^{13}C analysis, samples (~100 mg) were packed into 4 mm zirconium oxide rotors with Kel-F rotor caps. ^{13}C cross polarization with magic angle spinning (CP-MAS) NMR spectra were acquired using a Bruker Avance III 500 MHz spectrometer (Bruker Biospin, Canada) equipped with a Bruker 4 mm H-X MAS probe. Spectra were acquired with a spinning rate of 13 KHz, a ramp-CP contact time of 1 ms, a 1 s recycle delay, 71680 scans, 1024 time domain points at 298 K and ^1H decoupling using the Spinal64 decoupling scheme. Spectra were processed with a filling factor of 2 and exponential multiplication resulting in a line broadening of 20 Hz in the final transformed spectrum.

3.3.4 ^1H High-Resolution-Magic Angle Spinning (HR-MAS) NMR spectroscopy

^1H HR-MAS NMR spectra were acquired using a Bruker 500 MHz Avance spectrometer fitted with a 4-mm triply tuned ^1H - ^{13}C - ^{15}N HR-MAS probe fitted with an actively shielded Z gradient at a spinning speed of 6.666 KHz. ^1H spectra were acquired with 8192 time domain points and utilizing using a single Hahn echo corresponding to a total delay of 150 μs (one rotor period) prior to acquisition to suppress probe background. The ^1H spectra were apodized through multiplication with an exponential decay corresponding to 5 Hz line broadening in the transformed spectra, and a zero-filling factor of 2. ^1H Diffusion Edited Experiments were acquired with a bipolar pulse longitudinal encode-decode sequence. Scans (2048) were collected using a 1.5 ms, 333 mT m^{-1} sine shaped gradient pulse, a diffusion time of 30 ms, 8192 time domain points and a sample temperature of 298 K. The spectra were processed with a zero-filling factor of 2 and an exponential multiplication, which resulted in a line broadening of 10 Hz in the transformed spectrum. In essence the “editing” was optimized to permit the strongest diffusion filtering possible while minimizing signal loss through relaxation. As a result the more rigid components dominate the transformed spectrum while mobile components are attenuated.

3.3.5 ^1H - ^{13}C Heteronuclear Single Quantum Coherence (HSQC) spectroscopy

Samples (~30 mg) were placed in a 4-mm Zirconium Oxide Rotor and 60 μL of DMSO- d_6 was added as a swelling solvent. After homogenization of the sample using a stainless steel mixing rod, the rotor was doubly sealed using a Kel-F seal and a Kel-F

rotor cap. ^1H - ^{13}C HSQC spectra were collected in phase sensitive mode using Echo/Antiecho-TPPI gradient selection but without sensitivity enhancement to reduce additional relaxation from the second retro-INEPT block. Scans (3440) were collected for each of the 128 increments in the F1 dimension. 1024 data points were collected in F2, a $1\text{J } ^1\text{H}$ - ^{13}C (145Hz), rotor synchronized adiabatic swept pulses were used for inversion, refocusing and decoupling of the carbon nuclei throughout. For HSQC spectra the F2 dimension was multiplied by an exponential function corresponding to a 15 Hz line broadening and a zero-filling factor of 2. The F1 dimension was processed using a negative line broadening of 1Hz in combination with a Gaussian multiplication of 0.0007 and a zero-filled by a factor of 2.

3.3.6 Ruthenium tetroxide oxidation

The treatment was adapted from a previously published method (Blokker *et al.*, 2006). In short, equivalent sample mass corresponding to 5 mg of carbon was added to a 30-mL Teflon® centrifuge tube along with 2 mL of chloroform (CHCl_3), 2mL of acetonitrile (ACN) and 4 mL of 2M sodium iodate (NaIO_4). The mixture was homogenized by sonication for 5 minutes and 6 mg of ruthenium(III) chloride was added to the sample. The centrifuge tube was then shaken overnight (8 hours). Following shaking, 3 mL of ultrapure water and 2 mL of hexane were added. The internal standard, deuterated pentadecanoic acid, was then added to achieve a final concentration of $50 \mu\text{g mL}^{-1}$. The solution was vortexed then centrifuged to isolate the supernatant. The solution was then extracted once with hexane and twice with DCM, and the resulting extract was passed through a $0.7\text{-}\mu\text{m}$ glass fiber filter to remove residual ruthenium salts.

Exactly 0.5 mL of 5% aqueous sodium thiosulphate ($\text{Na}_2\text{S}_2\text{O}_3$) was then added in order to quench the oxidation reaction by scavenging any residual oxidant. The organic and aqueous phases of the resulting solution were then allowed to separate. The organic phase was isolated and the solvent was evaporated under a gentle stream of N_2 so that the residue could be esterified using a 10% BF_3 in MeOH solution. The mixture was heated for 2 hours at 100°C , quenched with 2 mL 5% aqueous sodium chloride, and extracted with hexane. The extract was dried and re-dissolved in DCM for analysis using a gas chromatograph (GC) coupled to a mass spectrometer (MS) or fitted with flame ionization detection (FID) for identification and quantitation. In addition to the natural samples, an experimental blank and triplicates of an in-house laboratory standard sediment from the Saguenay Fjord (QC) were oxidized, derivatized and analyzed to check for contamination, reproducibility and precision.

3.3.7 GC-MS and GC-FID analyses

Gas chromatographic analysis of the alkanolic and alkandioic acids produced upon oxidation was performed on an Agilent 6890N instrument equipped with a FID, an on-column injector and a 25-m fused silica column coated with DB-5ms (0.2 mm ID; film thickness 0.33 μm). Helium was used as the carrier gas and the detector was maintained at 300°C . The oven was ramped from 45°C (hold 1 min) to 140°C ($15^\circ\text{C}/\text{min}$), 214°C ($4^\circ\text{C}/\text{min}$), 216°C ($0.5^\circ\text{C}/\text{min}$), 219°C ($4^\circ\text{C}/\text{min}$), 223°C ($0.5^\circ\text{C}/\text{min}$) and finally to 310°C ($10^\circ\text{C}/\text{min}$, hold 15 min).

GC-MS analysis was conducted on a Varian CP-3800 GC coupled to a Saturn 2200 ion trap, using an identical column, temperature program and carrier gas as on the

GC-FID to facilitate identification of the peaks of interest. Peak identification and calibration was done using commercially available fatty acid methyl esters standards (Supelco[®] 37 Component FAME mix, 10 mg/mL).

3.3.8 GC-C-IRMS analyses

The alkanolic and alkanedioic acids were also analyzed by GC-C-IRMS (gas chromatograph coupled to a combustion reactor and an Isoprime isotope ratio mass spectrometer) to obtain the $\delta^{13}\text{C}$ signature of individual compounds. The same type of GC column and temperature programming sequence, with a delay in timing to allow for CO_2 reference gas measurement on the mass spectrometer, was used to facilitate compound identification. The combustion reactor was a 50-cm long quartz tube (0.5 mm OD) filled with copper oxide chips and kept at 850°C to oxidize individual peaks into CO_2 . In-house $\delta^{13}\text{C}$ calibration of a series of alkane standards (C_{14} , C_{16} , C_{18} , C_{21} , C_{23} and C_{26} ; >95 % purity) was carried out by combustion analysis using an Europa elemental analyzer coupled to an Isoprime isotope ratio mass spectrometer (EA-IRMS), and using the international isotopic calibration standard IAEA-C6 Sucrose ($\delta^{13}\text{C} = -10.45 \pm 0.03\text{‰}$). These in-house standard isotopic signatures were further verified against a GC-amenable certified C_{36} standard ($-30.00 \pm 0.04 \text{‰}$; Alex Sessions' laboratory, Indiana University) using an Agilent 6890N GC coupled to the IRMS (GC-C-IRMS).

Results & Discussion

3.4.1 Abundance of the NHOM fraction

The nine samples studied in this work were chemically separated into three chemical reactivity classes: (i) lipid-like organic solvent soluble OM, (ii) acid soluble + hydrolyzable material, and (3) non-hydrolyzable + refractory OM (Chapter II). Between 23.9 and 54.0% of total organic carbon was found in this last fraction, with a trend of increasing relative abundance seaward and with depth in the sediment. Noteworthy, despite a similar chemical composition in both terrestrially influenced and marine samples, the $\delta^{13}\text{C}$ and $\delta^{15}\text{N}$ signatures of the NHOM fraction are more enriched with distance from the river mouth moving offshore, suggesting different sources for chemically similar organic compounds. Given the quantitative importance of the NHOM fraction in sediment, more details are needed on its chemical composition and structure to understand its origin, formation pathway and fate under different conditions.

3.4.2 Structural analysis of NHOM

The solid state ^{13}C NMR spectrum of the NHOM residues (Figure 3.1) was dominated by a peak at 30 ppm, corresponding to methylenic carbon found in polymethylene chains.

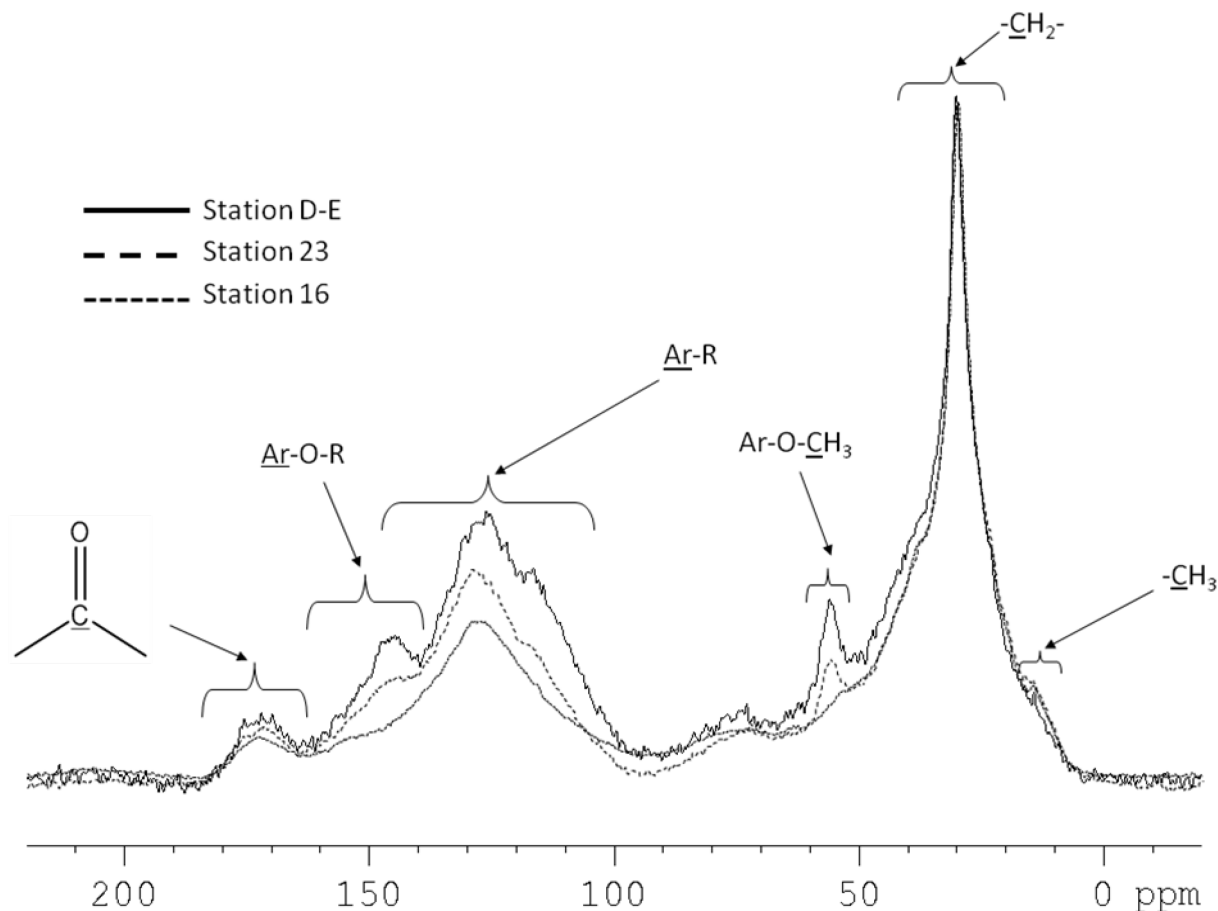


Figure 3.1 Schematic Solid-state ^{13}C CP-MAS NMR of the fresh, mixed, and salt-water samples.

The small shoulder at 15 ppm, slightly increasing in intensity with samples that were farther offshore, is derived from terminal methyl groups. An aromatic signal, centered between 110-140 ppm, in conjunction with both methoxy and aromatic-bound ether signals centered at 55 and 145 ppm, respectively, suggest a contribution from lignin (Mathers *et al.*, 2007), with a possible minor contribution from other aromatic compounds belonging to the refractory OM component. The close correlation of these three peaks however suggests that a lignin signal predominates in these regions of the spectrum, and that the relative contribution of lignin to the NHOM fraction decreases seaward from the river mouth.

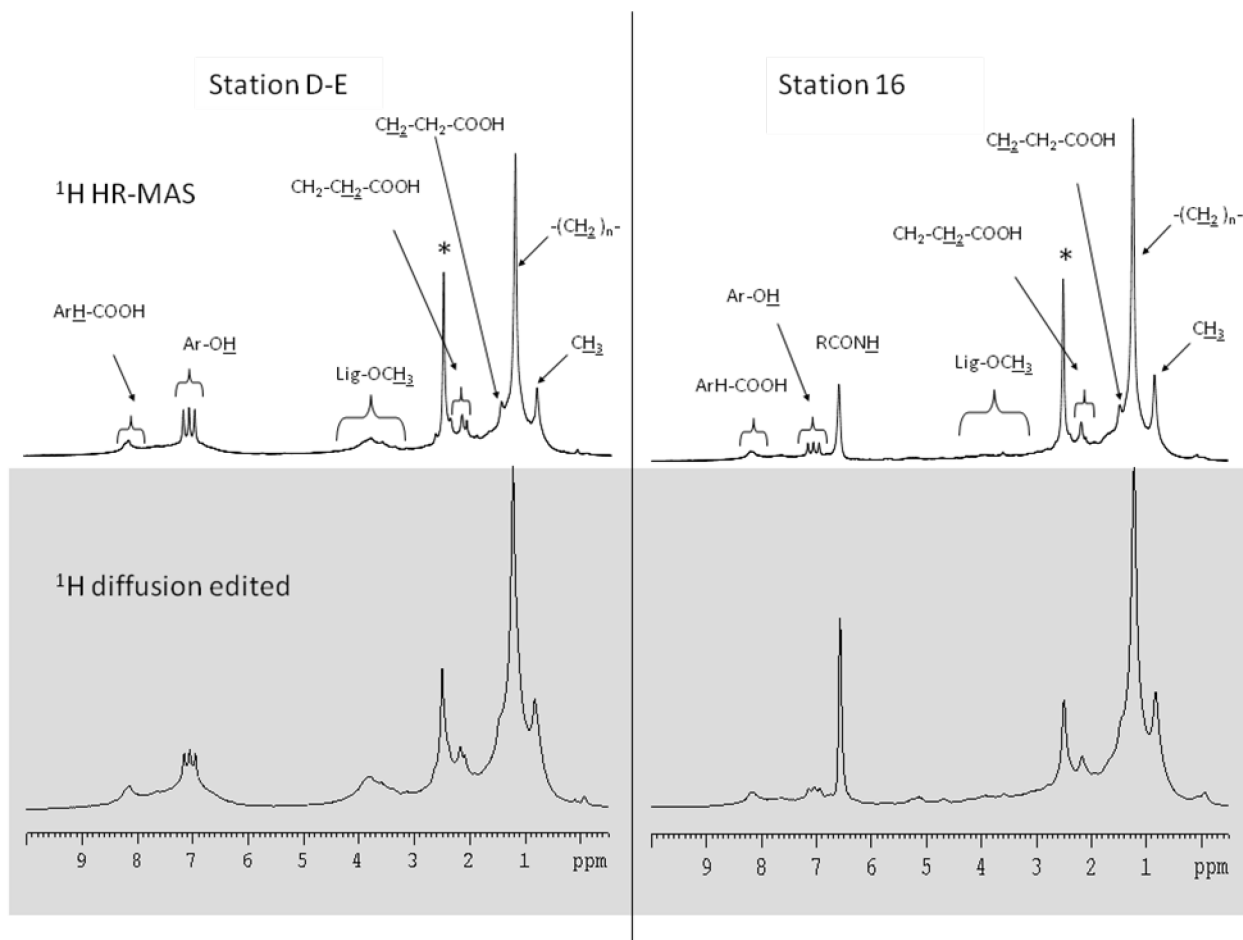


Figure 3.2 ^1H HR-MAS (top) and ^1H diffusion edited (bottom) NMR spectra of the fresh (Station DE) and salt water (Station 16) samples. The asterisk corresponds to the locking standard DMSO-d₆.

Structural assignment was further corroborated using ^1H HR-MAS NMR spectroscopy. Figure 3.2 shows a predominant contribution from polymethylene chains, centered at 1.3 ppm, with an aromatic signal, centered at 7.2 ppm, which is again decreasing offshore. The signal was diffusion edited; the resulting decrease in aliphatic signal revealed a slightly more pronounced signal for aromatic moieties in the terrestrial sample and exchangeable amide protons, centered at 6.5 ppm, in the marine sample. The

latter agrees with the higher proportion of total nitrogen found in the NHOM fraction of marine samples compared to the terrestrial sampling sites (Chapter II).

Two dimensional ^1H - ^{13}C HSQC NMR analysis (Figure 3) was also conducted on the NHOM residue isolated from the Station D-E sample to better resolve the overlapping peaks in the aliphatic and the methoxy regions of the spectrum. Once again, the 2D plot shows a predominant aliphatic signal which can be deconvoluted into terminal methyl, methylenic, as well as CH_2 groups in the alpha and beta position of a carboxyl. These peaks suggest the presence of fatty acid-like compounds condensed in large macrobiopolymers that are not soluble in organic solvents (Chapter II). Using 2D NMR also allows two low intensity chemical shifts to be distinguished: terminal hydroxyl groups attached to a methylenic carbon, 3.7×65 ppm, as well as ester bound CH_2 groups, 4×70 ppm (Simpson *et al.*, 2003).

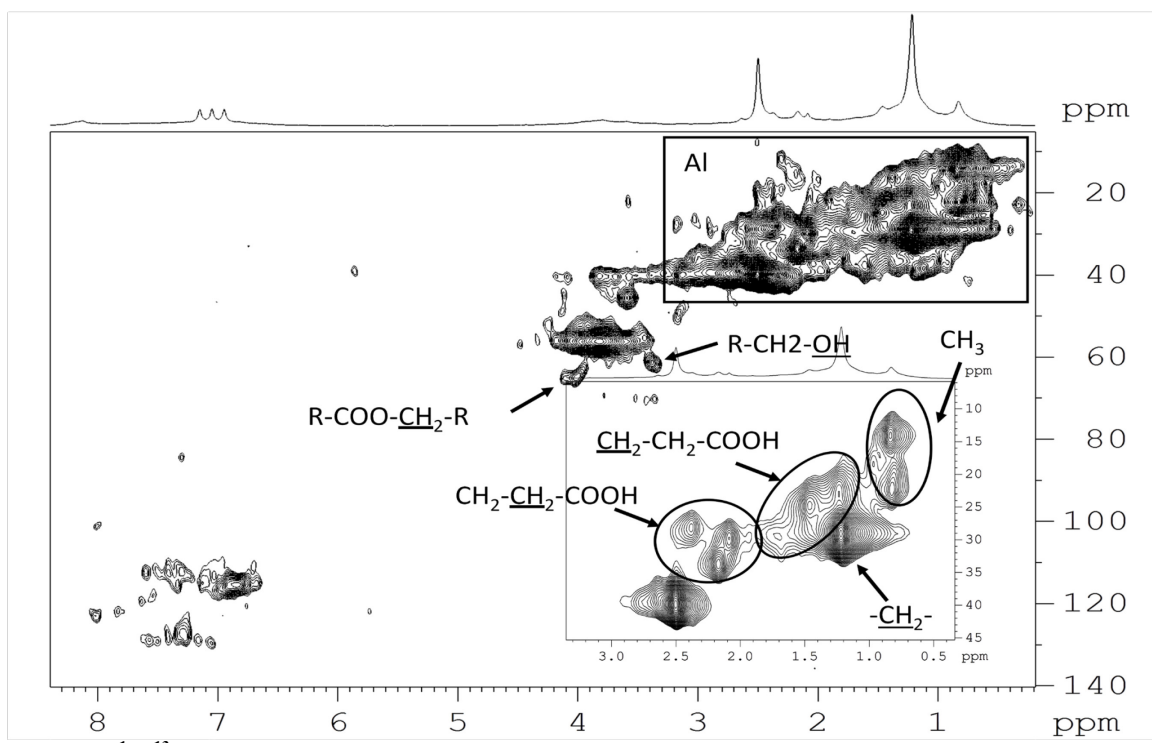


Figure 3.3 ^1H - ^{13}C HSQC of the freshwater surface sample. The aliphatic region (Al) is expanded in the insert.

3.4.3 RuO₄ Oxidation products

To find clues on the structure of the NHOM fraction in terrestrial, mixed and marine samples, the RuO₄ oxidation method (Blokker *et al.*, 1998) was applied to the untreated sediment samples and their NHOM isolate for the surface sample at the four sampling sites (Figures 3.4a and 3.4b). Two major families of oxidation products were generated, namely a series of C₄-C₃₀ alkanolic acids and a series of C₇-C₂₇ alkandioic acids. Although identification of the compounds was possible, the C₄-C₆ alkanolic and alkandioic acids were not considered further in the discussion or calculations because they are highly volatile when derivatized; it is therefore assumed the low relative abundances found for these short-chain acids reflect partial sample loss during sample preparation. All raw sediment samples showed a maximum for alkanolic acids at C₁₈ followed by C₁₆ and C₁₅; corresponding to algal and bacterial OM contributions (Kawamura *et al.*, 1987). A second series of peaks from C₂₀ to C₃₀ and centered around C₂₂ to C₂₄ indicates a contribution from terrestrial fatty acids at all sites (Bourbonniere & Meyers, 1996), with a decreasing relative importance seaward. As a result, the distribution of the saturated alkanolic acids shifts toward shorter chain lengths moving offshore, corresponding to a change in OM inputs, from a mix of terrestrial and bacterial matter to a mix of algal and bacterial OM; an observation mirrored by isotope results presented in Chapter II (Table 2.2). Hayes (1993) showed seaward enrichment of OC resulting from the utilization of bicarbonate as the carbon source. These differences are emphasized even more in the NHOM fraction (Figure 3.4b), although with greater variability. An even stronger predominance of shorter chain alkanolic acids is found in the

marine samples (Station 16), while the longer chain alkanolic acids predominate in the terrestrial samples (Lake Jean, but even more strikingly at Station D-E).

The integrative parameter TAR (terrestrial-to-aquatic ratio) value calculated for each sample corresponds to the ratio of the sum of the concentrations measured for the long chain alkanolic acids (C_{19} to C_{30}) to that of the short chain alkanolic acids (C_7 to C_{18}). High TAR values thus indicate sample with higher relative terrestrial OM inputs, while low values are typical of marine samples (Cooper & Bray, 1963). Figure 3.5 shows the variations in TAR plotted as a function of the distance from mouth of the St. Lawrence River.

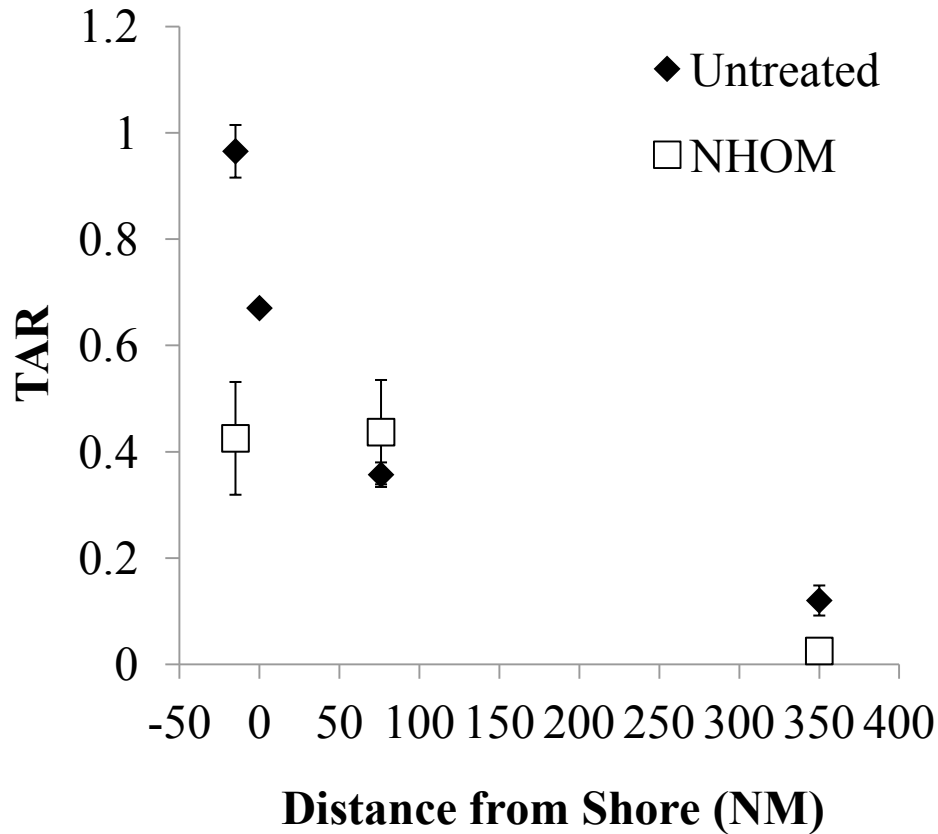


Figure 3.5 The terrestrial vs. aquatic ratio (TAR) shows a clear relationship between chain length preference and distance from the mouth of the SLE for alkanolic acids liberated from untreated sediments and their NHOM residues

In addition to a clear decrease of chain length with distance from the mouth of the estuary, clear differences were found in the carbon preference index (CPI) values; (preference of even-chain molecules over odd-chain ones, or carbon preference index (Cooper & Bray, 1963). CPI values > 2.5 represent fresh OM while < 1 correspond to ancient and/or reprocessed OM. The values measured in this study ranged from 0.18 to 1.88 for the oxidation products from untreated sediment and 0.18 to 0.86 for those obtained for the NHOM residues (Figure 3.6); suggesting OM being deposited is more degraded moving offshore. Most untreated samples contained fresher OM compared to their NHOM isolates (the reason for the much lower value measured at Station 16, 0-5 cm, is unknown), suggesting that the NHOM isolates are composed of highly processed OM or that the building blocks of the macrobiopolymer structure are even-chain aliphatic compounds.

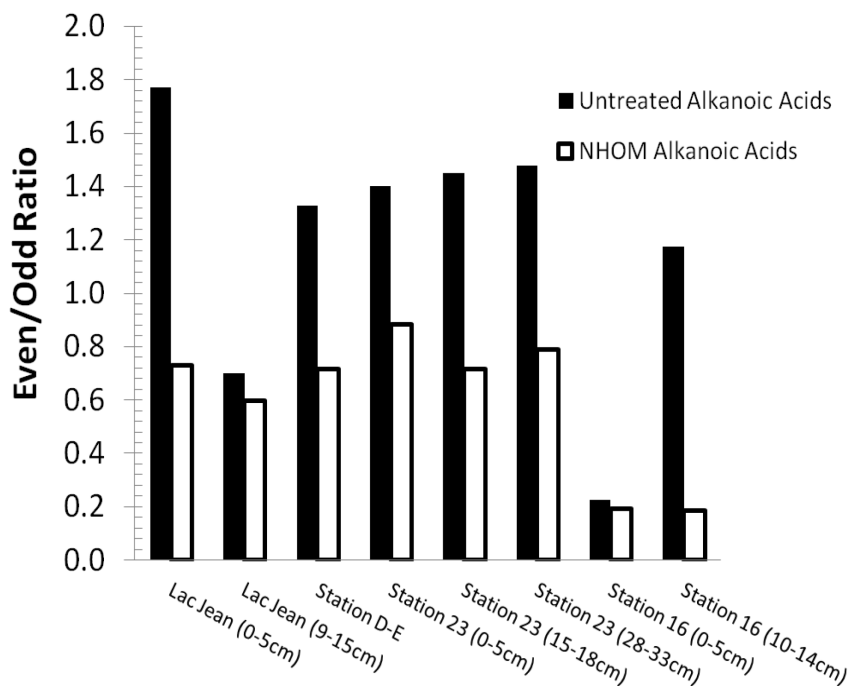


Figure 3.6 Carbon preference index (CPI) values show a clear difference in the even-to-odd ratios calculated for the untreated samples and their isolates

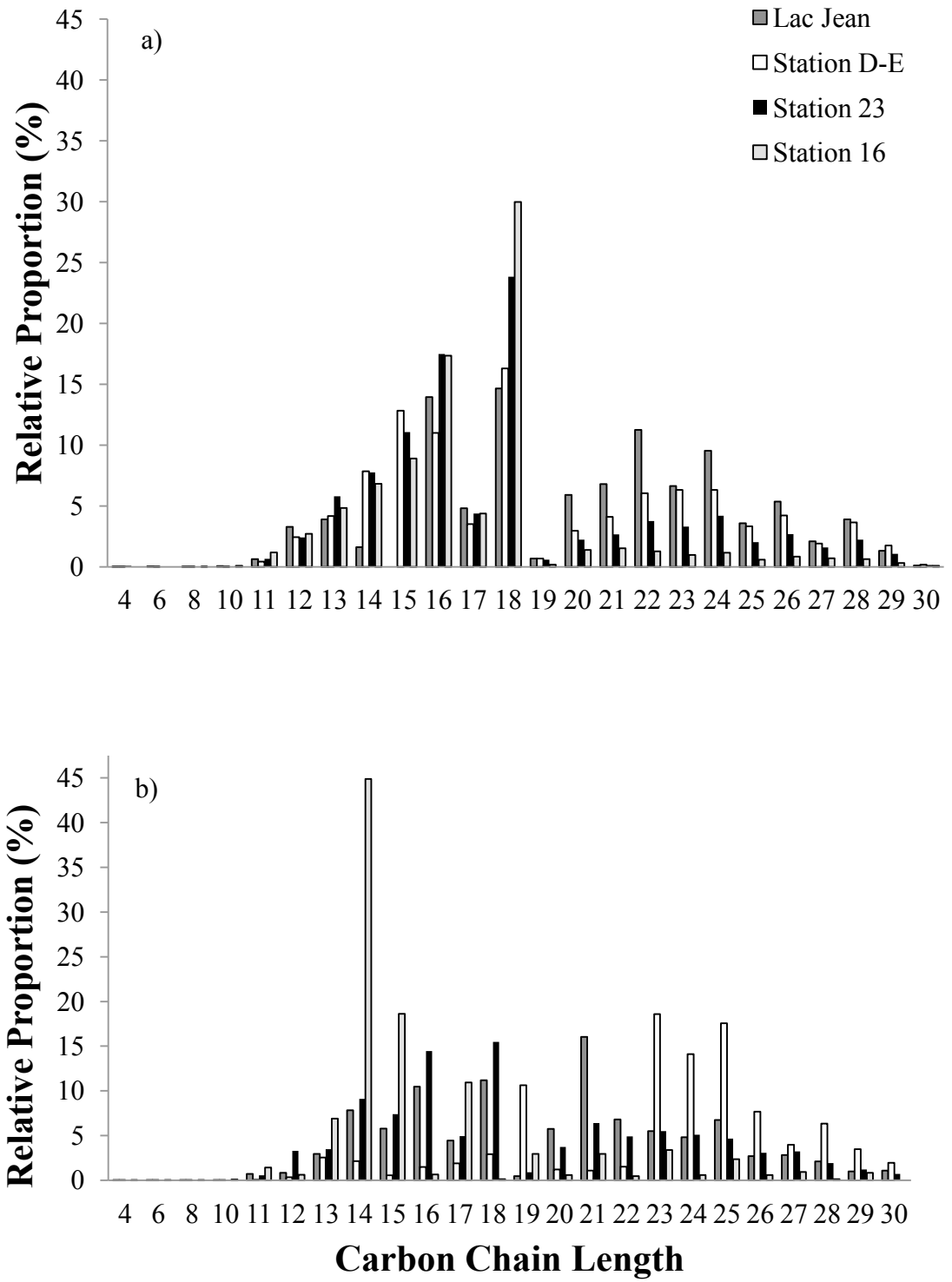


Figure 3.4 Alkanolic acids liberated from (a) raw sediments and (b) the NHOM isolate for lacustrine (Lake Jean), fresh (Stn DE), mixed (Stn 23) and salt-water (Stn 16) samples

Table 3.1 Quantification of alkanolic acids from RuO₄ treatment

| #C | Lac Jean (0-3cm) | | Lac Jean (9-15cm) | | Station D-E | | Station 23 (0-5cm) | | Station 23 (15-18cm) | | Station 23 (28-33cm) | | Station 16 (0-5cm) | | Station 16 (10-14cm) | | |
|-----------------|------------------|-------|-------------------|-------|-------------|-------|--------------------|-------|----------------------|-------|----------------------|-------|--------------------|-------|----------------------|-------|-------|
| | Untreated | NHOM | Untreated | NHOM | Untreated | NHOM | Untreated | NHOM | Untreated | NHOM | Untreated | NHOM | Untreated | NHOM | Untreated | NHOM | |
| Alkanolic Acids | 4 | 0.01 | 0.01 | 0.24 | 0.02 | 0.00 | 0.03 | 0.08 | 0.01 | 0.09 | 0.03 | 0.02 | N.D. | N.D. | 0.01 | N.D. | 0.01 |
| (% of Total) | 6 | 0.03 | 0.02 | 0.01 | 0.00 | 0.01 | 0.01 | N.D. | 0.03 | 0.06 | 0.02 | 0.02 | 0.03 | N.D. | 0.00 | 0.01 | 0.00 |
| | 8 | 0.00 | 0.01 | 0.00 | 0.00 | 0.01 | 0.02 | 0.02 | 0.01 | 0.01 | 0.00 | 0.00 | 0.00 | 0.01 | 0.01 | 0.00 | 0.03 |
| | 10 | 0.06 | 0.00 | 0.01 | 0.01 | 0.01 | 0.01 | 0.01 | 0.02 | 0.04 | 0.01 | 0.02 | 0.01 | 0.07 | 0.09 | N.D. | 0.22 |
| | 11 | 0.63 | 0.72 | 0.20 | 0.84 | 0.43 | 0.07 | 0.64 | 0.56 | 1.12 | 0.41 | 0.64 | 0.22 | 1.17 | 1.44 | 0.42 | 2.17 |
| | 12 | 3.29 | 0.84 | 1.84 | 4.32 | 2.43 | 0.35 | 2.41 | 3.28 | 3.52 | 2.91 | 2.92 | 1.60 | 2.71 | 0.62 | 2.66 | 0.85 |
| | 13 | 3.89 | 2.94 | 2.51 | 2.54 | 4.18 | 2.55 | 5.80 | 3.46 | 6.12 | 3.13 | 4.65 | 2.60 | 4.83 | 6.88 | 7.33 | 6.92 |
| | 14 | 1.62 | 7.83 | 6.33 | 7.71 | 7.84 | 2.13 | 7.76 | 9.10 | 7.38 | 8.46 | 7.60 | 6.63 | 6.83 | 44.90 | 10.38 | 45.99 |
| | 15 | N.D. | 5.78 | 7.00 | 4.18 | 12.82 | 0.55 | 11.09 | 7.38 | 9.97 | 6.61 | 9.55 | 6.35 | 8.89 | 18.62 | 15.70 | 16.41 |
| | 16 | 13.95 | 10.46 | 7.31 | 10.06 | 11.00 | 1.48 | 17.50 | 14.44 | 16.14 | 13.43 | 17.18 | 12.84 | 17.36 | 0.64 | 17.11 | 0.89 |
| | 17 | 4.80 | 4.43 | 3.09 | 3.63 | 3.51 | 1.88 | 4.37 | 4.95 | N.D. | 4.91 | 3.75 | 5.12 | 4.38 | 10.93 | 8.31 | 11.39 |
| | 18 | 14.66 | 11.17 | 8.34 | 12.23 | 16.31 | 2.92 | 23.86 | 15.49 | 29.02 | 14.53 | 25.97 | 15.51 | 29.98 | 0.13 | 22.22 | 0.13 |
| | 19 | 0.67 | 0.47 | 0.31 | 0.58 | 0.67 | 10.62 | 0.59 | 0.88 | 0.68 | 0.93 | 0.76 | 0.85 | 0.18 | 2.96 | 0.40 | 3.24 |
| | 20 | 5.90 | 5.76 | 4.00 | 4.65 | 2.97 | 1.19 | 2.24 | 3.73 | 1.66 | 3.98 | 2.23 | 4.58 | 1.37 | 0.60 | 2.35 | 0.80 |
| | 21 | 6.79 | 16.05 | 4.89 | 18.24 | 4.11 | 1.07 | 2.67 | 6.40 | 2.51 | 7.87 | 2.88 | 8.29 | 1.53 | 2.96 | 2.86 | 2.70 |
| | 22 | 11.24 | 6.80 | 8.81 | 5.79 | 6.05 | 1.51 | 3.77 | 4.91 | 3.60 | 4.97 | 3.52 | 5.93 | 1.26 | 0.47 | 1.90 | 0.52 |
| | 23 | 6.64 | 5.49 | 4.91 | 4.20 | 6.32 | 18.59 | 3.31 | 5.51 | 3.32 | 5.78 | 3.18 | 6.77 | 0.98 | 3.39 | 1.73 | 2.99 |
| | 24 | 9.54 | 4.81 | 7.69 | 4.24 | 6.33 | 14.12 | 4.20 | 5.08 | 4.39 | 5.23 | 3.93 | 6.79 | 1.16 | 0.58 | 1.95 | 0.66 |
| | 25 | 3.57 | 6.73 | 2.73 | 5.73 | 3.33 | 17.56 | 2.03 | 4.67 | 2.21 | 6.23 | 2.24 | 11.19 | 0.59 | 2.35 | 1.00 | 2.13 |
| | 26 | 5.36 | 2.71 | 4.02 | 2.11 | 4.22 | 7.67 | 2.70 | 3.08 | 3.01 | 2.53 | 3.14 | 4.74 | 0.84 | 0.58 | 1.38 | 0.18 |
| | 27 | 2.09 | 2.83 | 22.43 | 5.48 | 1.91 | 3.99 | 1.58 | 3.24 | 1.68 | 4.33 | 1.49 | N.D. | 14.85 | 0.94 | 0.85 | 0.86 |
| | 28 | 3.89 | 2.11 | 2.70 | 1.44 | 3.65 | 6.34 | 2.24 | 1.93 | 2.57 | 1.68 | 3.07 | N.D. | 0.63 | 0.11 | 0.82 | 0.14 |
| | 29 | 1.31 | 0.98 | 0.77 | 0.58 | 1.75 | 3.47 | 1.06 | 1.20 | 0.96 | 1.15 | 1.05 | N.D. | 0.30 | 0.83 | 0.37 | 0.80 |
| | 30 | 0.09 | 1.10 | 0.11 | 1.45 | 0.17 | 1.96 | 0.16 | 0.70 | 0.11 | 0.93 | 0.22 | N.D. | 0.07 | N.D. | 0.28 | N.D. |
| Sum (mg/g C) | | 17.62 | 1.42 | 0.71 | 1.17 | 0.36 | 11.49 | 0.28 | 0.53 | 0.16 | 0.77 | 0.25 | 0.71 | 0.68 | 71.62 | 0.32 | 68.51 |
| CPI | | 1.77 | 0.73 | 0.70 | 0.60 | 1.33 | 0.72 | 1.40 | 0.88 | 1.45 | 0.72 | 1.48 | 0.79 | 0.23 | 0.19 | 1.17 | 0.19 |
| TAR | | 1.00 | 0.50 | 0.93 | 0.35 | 0.67 | 0.00 | 0.33 | 0.38 | 0.37 | 0.38 | 0.37 | 0.55 | 0.10 | 0.03 | 0.14 | 0.02 |

Table 3.1 (cont.) Quantification of alkanedioic acids from RuO₄ treatment

| #C | Lac Jean (0-3cm) | | Lac Jean (9-15cm) | | Station D-E | | Station 23 (0-5cm) | | Station 23 (15-18cm) | | Station 23 (28-33cm) | | Station 16 (0-5cm) | | Station 16 (10-14cm) | | |
|------------------|------------------|-------|-------------------|-------|-------------|-------|--------------------|-------|----------------------|-------|----------------------|-------|--------------------|-------|----------------------|-------|-------|
| | Untreated | NHOM | Untreated | NHOM | Untreated | NHOM | Untreated | NHOM | Untreated | NHOM | Untreated | NHOM | Untreated | NHOM | Untreated | NHOM | |
| Alkandioic Acids | 7 | 0.29 | 1.73 | 1.75 | 1.13 | 3.89 | 0.30 | 4.17 | 2.27 | 3.53 | 2.89 | 2.09 | N.D. | 2.07 | 5.87 | 1.71 | 2.83 |
| (% of Total) | 8 | 0.04 | 3.79 | 0.48 | 5.51 | 0.76 | 0.33 | 1.23 | 2.60 | 0.79 | 4.59 | 0.88 | N.D. | 0.98 | N.D. | 2.48 | N.D. |
| | 9 | N.D. | N.D. | N.D. | N.D. | N.D. | N.D. | N.D. | N.D. | N.D. | N.D. | N.D. | N.D. | N.D. | 0.03 | N.D. | 0.05 |
| | 10 | 0.00 | 0.03 | 0.02 | 0.03 | 0.01 | 0.05 | 0.08 | 0.02 | N.D. | 0.04 | 0.02 | 0.10 | 0.05 | N.D. | N.D. | 0.49 |
| | 11 | 0.07 | 1.54 | 0.36 | 0.51 | 0.25 | 1.94 | 0.90 | 0.60 | 1.22 | 0.36 | 0.61 | 0.66 | 10.55 | 0.67 | N.D. | 2.82 |
| | 12 | 0.54 | 2.72 | 2.41 | 0.93 | 4.20 | 0.46 | 5.54 | 1.18 | 4.63 | 0.79 | 2.85 | 1.05 | 2.57 | 5.12 | 0.86 | 3.53 |
| | 13 | 9.03 | 6.52 | 7.02 | 7.21 | 4.41 | 5.77 | 11.59 | 7.55 | 11.05 | 8.41 | 5.57 | 7.16 | 20.11 | 25.09 | 20.29 | 15.94 |
| | 14 | 78.22 | 4.84 | 7.07 | 7.87 | 5.01 | 47.30 | 22.00 | 8.72 | 18.05 | 8.39 | 9.18 | 9.79 | 29.25 | 3.15 | 34.90 | 1.02 |
| | 15 | 1.08 | 0.80 | 2.60 | 20.28 | 3.57 | 18.19 | 16.74 | 1.23 | 24.61 | 6.14 | 2.77 | 6.01 | 2.84 | 13.70 | 5.11 | 13.21 |
| | 16 | 0.43 | 3.06 | 2.65 | 3.28 | 2.23 | 0.06 | 1.70 | 3.22 | 1.15 | 3.70 | 2.71 | 3.49 | 1.39 | 1.86 | 1.66 | 3.21 |
| | 17 | 1.58 | 9.20 | 12.81 | 9.84 | 7.92 | 12.20 | 5.41 | 8.39 | 0.70 | 8.43 | 10.29 | 8.15 | 5.17 | 13.18 | 6.99 | 12.01 |
| | 18 | 0.64 | 4.78 | 5.73 | 4.28 | 3.70 | 0.12 | 3.28 | 5.53 | 3.08 | 6.42 | 5.59 | 6.62 | 3.26 | 2.36 | 3.73 | 4.59 |
| | 19 | 1.58 | 17.32 | 11.25 | 7.30 | 13.06 | 3.29 | 4.76 | 14.42 | 6.98 | 13.84 | 13.14 | 13.17 | 2.94 | 5.39 | 5.01 | 8.11 |
| | 20 | 0.40 | 5.06 | 3.27 | 5.09 | 3.29 | 2.15 | 1.21 | 4.85 | 0.25 | 3.49 | 3.89 | 4.19 | 2.58 | 1.40 | 1.53 | 0.30 |
| | 21 | 0.38 | 1.78 | 2.87 | 1.16 | 3.72 | 4.89 | 5.91 | 1.95 | 7.11 | 3.55 | 2.54 | 3.15 | 4.86 | 4.43 | 4.64 | 7.07 |
| | 22 | 0.64 | 2.84 | 4.54 | 2.74 | 4.13 | 0.05 | 3.45 | 3.63 | 2.39 | 3.41 | 4.06 | 3.91 | 1.09 | 1.41 | 2.03 | 3.19 |
| | 23 | 1.49 | 10.16 | 9.81 | 5.73 | 9.95 | 0.77 | 3.37 | 8.74 | 0.71 | 6.78 | 9.50 | 9.32 | 1.76 | 5.37 | 3.13 | 6.47 |
| | 24 | 0.62 | 2.69 | 4.12 | 2.57 | 4.41 | 0.22 | 1.70 | 3.34 | 1.82 | 2.57 | 4.81 | 4.07 | 0.87 | 0.29 | 1.64 | 2.54 |
| | 25 | 2.00 | 13.93 | 13.79 | 8.42 | 15.38 | 1.16 | 4.11 | 12.17 | 8.96 | 9.52 | 11.05 | 15.19 | 1.44 | 4.41 | 1.80 | 4.98 |
| | 26 | 0.39 | 2.16 | 3.56 | 2.03 | 3.18 | 0.15 | 1.20 | 2.92 | 1.26 | 2.23 | 3.18 | 3.98 | 4.79 | 1.96 | 1.16 | 2.65 |
| | 27 | 0.59 | 5.04 | 3.88 | 4.09 | 6.93 | 0.60 | 1.65 | 6.68 | 1.72 | 4.44 | 5.27 | N.D. | 1.44 | 4.31 | 1.33 | 5.02 |
| | Sum (mg/g C) | 44.99 | 0.45 | 0.18 | 0.34 | 0.09 | 74.92 | 0.04 | 0.16 | 0.02 | 0.17 | 0.07 | 0.15 | 0.06 | 5.72 | 0.04 | 10.95 |

3.4.4 Compound-specific $\delta^{13}\text{C}$ analysis of the RuO_4 oxidation products

Compound-specific $\delta^{13}\text{C}$ analysis was conducted on the alkanolic/dioic acids produced upon oxidation of the untreated samples and their isolates. Measurement of the carbon stable isotope signatures was possible only for compounds that were well resolved on the GC chromatograms and high enough in concentration. These compounds were the $\text{C}_{12}\text{-C}_{20}$ alkanolic acids and the $\text{C}_9\text{-C}_{20}$ alkanedioic acids (Table 3.2). The $\delta^{13}\text{C}$ signature obtained for alkanolic acids derived from both the untreated sediments and NHOM residues showed a seaward enrichment that paralleled the pattern obtained for the bulk samples (Chapter II). In addition to the enrichment offshore, isotopes of the long chain alkanolic acids displayed more depleted signatures compared to the shorter chain compounds, an observation that agrees with the hypothesis of the utilization of readily available materials during synthesis of the cell wall of phytoplankton organisms (Versteegh *et al.*, 2004). There was a nearly linear relationship between the $\delta^{13}\text{C}$ signatures of alkanolic acids from the untreated samples and those of the NHOM isolates (Figure 3.7), with differences in signatures for individual compounds stemming from the origin of the carbon source (more ^{13}C -depleted signatures for terrestrial OM and more enriched ones for marine OM; (Hayes, 1993). This relationship suggests a selective preservation pathway, as NHOM shows the same potential for preservation independent of its source. It appears that what determines whether an OM component is preserved and eventually buried in sediments is its chemical structure rather than origin.

The $\delta^{13}\text{C}$ signature of two alkanolic acids, C_{15} and C_{17} , differs significantly compared to those of the others compounds. While all other alkanolic acids showed enriching signatures going seaward and very close agreement between ^{13}C signatures of

untreated sediment and their NHOM isolates, the C₁₅ and C₁₇ alkanolic acids, which are both considered markers for bacterial OM sources and reprocessing (Gelin *et al.*, 1997), displayed more ¹³C enriched signatures in the NHOM isolates suggesting some level of bacterial reprocessing prior to incorporation into the NHOM component (Figure 3.8). In the NHOM residues, both acids displayed signatures enriching seaward, suggesting different sources for the lipid-like compounds integrated in NHOM components (Gelin *et al.*, 1994), however this observation requires further investigation.

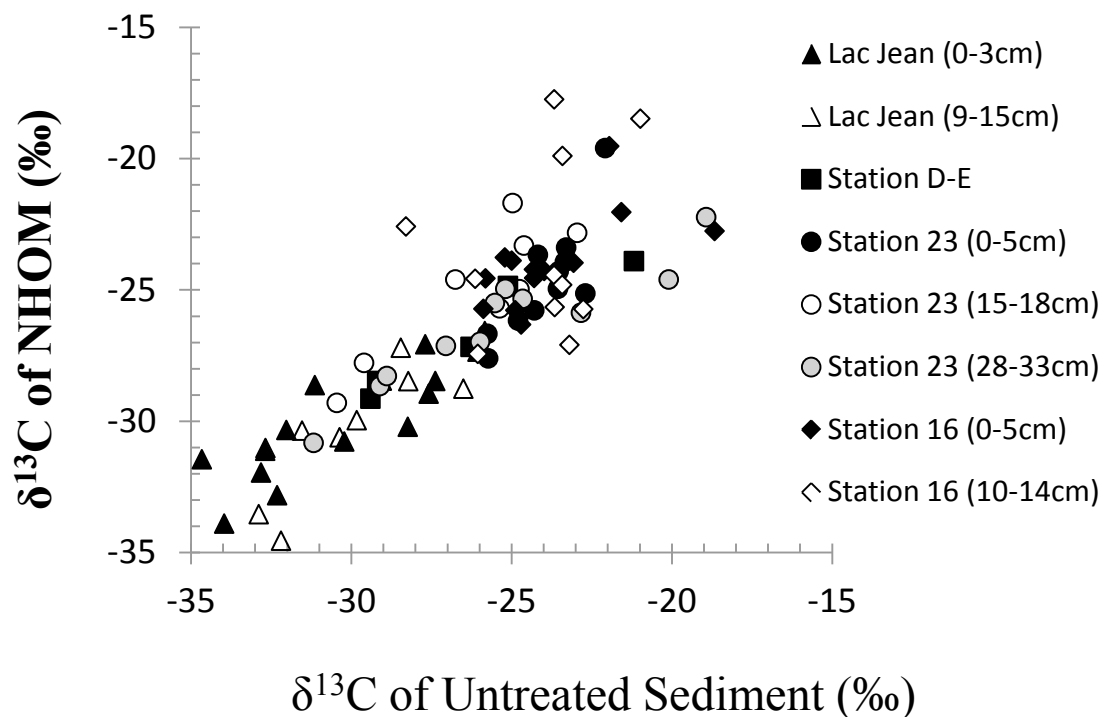


Figure 3.7 The comparison of the $\delta^{13}\text{C}$ stable isotope signature of alkanolic acids liberated from the untreated sediments and their NHOM isolates shows a nearly linear relationship reflecting the variations in relative contributions from terrestrial (lower $\delta^{13}\text{C}$ values)

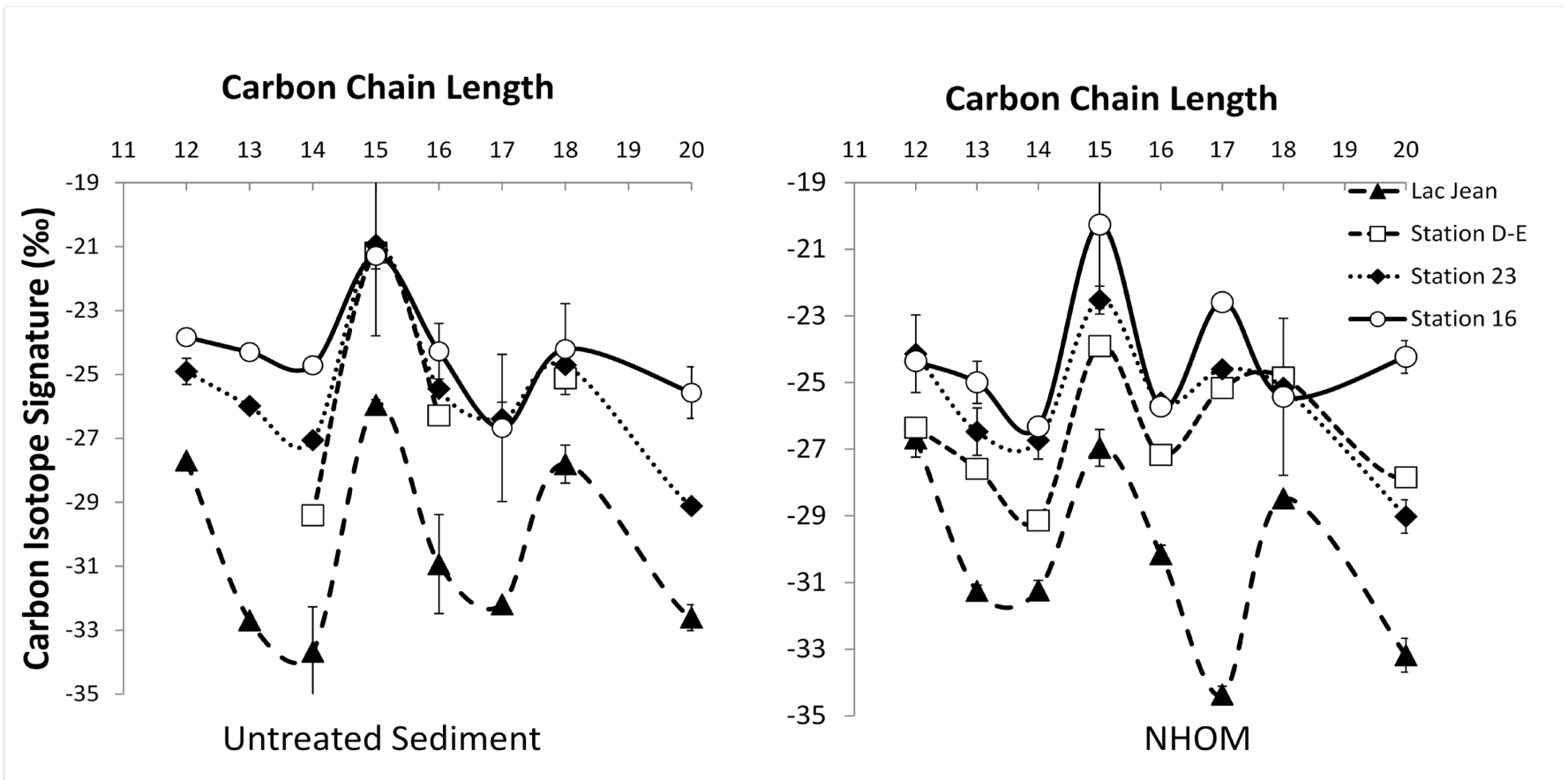


Figure 3.8 Compound-specific $\delta^{13}\text{C}$ stable isotope signatures of the alkanolic acids from (a) the untreated sediment and (b) their NHOM isolates.

Table 3.2. Compound-specific $\delta^{13}\text{C}$ analysis of the oxidation products from the RuO_4 treatment

| | #C | Lac Jean (0-3cm) | | Lac Jean (9-15cm) | | Station D-E | | Station 23 (0-5cm) | | Station 23 (15-18cm) | | Station 23 (28-33cm) | | Station 16 (0-5cm) | | Station 16 (10-14cm) | |
|------------------|----|------------------|--------|-------------------|--------|-------------|--------|--------------------|--------|----------------------|--------|----------------------|--------|--------------------|--------|----------------------|--------|
| | | Untreated | NHOM | Untreated | NHOM | Untreated | NHOM | Untreated | NHOM | Untreated | NHOM | Untreated | NHOM | Untreated | NHOM | Untreated | NHOM |
| Alkanoic Acids | 12 | -27.70 | -27.07 | n/a | -26.28 | n/a | -26.35 | -23.53 | -24.29 | -24.62 | -23.31 | -25.20 | -24.96 | -23.98 | -24.28 | -23.68 | -24.44 |
| (%) | 13 | -32.69 | -31.13 | n/a | -31.37 | n/a | -27.59 | -24.29 | -25.78 | n/a | -25.97 | -25.99 | -26.97 | -24.30 | -24.55 | n/a | -25.44 |
| | 14 | -34.66 | -31.45 | -32.68 | -31.02 | -29.41 | -29.14 | -24.80 | -26.17 | n/a | -26.34 | -27.05 | -27.13 | -24.70 | -26.32 | -24.72 | n/a |
| | 15 | -26.07 | -27.35 | -25.84 | -26.57 | -21.19 | -23.90 | -22.08 | -19.60 | -22.96 | -22.83 | -18.93 | -22.23 | -21.58 | -22.04 | -20.99 | -18.48 |
| | 16 | -32.03 | -30.33 | -29.83 | -29.96 | -26.28 | -27.17 | -23.56 | -24.96 | -25.37 | -25.70 | -25.52 | -25.50 | -24.89 | -25.77 | -23.66 | -25.65 |
| | 17 | n/a | -34.18 | -32.19 | -34.55 | n/a | -25.16 | -22.70 | -25.14 | -26.76 | -24.60 | -26.02 | n/a | -25.04 | n/a | -28.30 | -22.58 |
| | 18 | -27.38 | -28.47 | -28.22 | -28.47 | -25.12 | -24.85 | -23.34 | -23.93 | -24.76 | -24.97 | -24.66 | -25.34 | -25.21 | -23.76 | -23.20 | -27.09 |
| | 20 | -32.32 | -32.82 | -32.89 | -33.54 | n/a | -27.84 | -25.76 | -26.67 | n/a | -29.37 | -29.11 | -28.66 | -25.00 | -23.89 | -26.14 | -24.58 |
| | 21 | -30.77 | n/a | -31.02 | n/a | n/a | -23.13 | n/a | -23.52 | n/a | -12.09 | -29.13 | n/a | n/a | n/a | n/a | n/a |
| | 22 | -30.89 | n/a | -31.19 | n/a | n/a | n/a | n/a | -24.73 | n/a | n/a | n/a | n/a | -21.82 | n/a | n/a | n/a |
| | 23 | -31.14 | -28.63 | -31.30 | n/a | n/a | n/a | n/a | n/a | n/a | n/a | -29.72 | n/a | n/a | n/a | n/a | n/a |
| | 24 | n/a | n/a | -30.37 | -30.61 | -29.19 | -28.47 | -25.73 | -27.61 | -29.61 | -27.78 | n/a | -30.05 | -25.82 | -24.56 | n/a | n/a |
| Alkandioic Acids | 9 | n/a | -29.17 | n/a | -29.08 | n/a | -27.08 | n/a | -24.60 | n/a | n/a | n/a | n/a | -24.53 | n/a | n/a | -26.44 |
| (%) | 10 | -28.24 | -30.21 | n/a | -30.42 | n/a | -26.64 | -23.30 | -23.39 | n/a | -25.66 | -22.84 | -25.87 | -23.07 | -23.97 | -23.42 | -24.81 |
| | 11 | -38.83 | n/a | n/a | -38.67 | n/a | -31.42 | -24.26 | n/a | n/a | -24.59 | -20.10 | -24.60 | -24.31 | -24.22 | -23.67 | -17.74 |
| | 12 | -32.82 | -31.96 | -29.39 | n/a | n/a | -25.35 | -24.18 | -23.66 | -24.97 | -21.69 | -24.15 | n/a | -24.29 | n/a | -22.77 | -25.73 |
| | 13 | n/a | -18.55 | -26.51 | -28.76 | n/a | -24.67 | n/a | -21.58 | n/a | n/a | -21.62 | n/a | -21.95 | -19.53 | -23.42 | -19.90 |
| | 14 | -29.05 | -28.45 | -31.54 | -30.36 | n/a | -21.77 | n/a | -23.57 | n/a | -21.93 | -25.10 | n/a | n/a | n/a | n/a | n/a |
| | 15 | n/a | n/a | -31.81 | n/a | n/a | n/a | n/a | -22.99 | n/a | n/a | n/a | n/a | -18.67 | -22.76 | n/a | n/a |
| | 16 | -27.59 | -28.95 | -28.46 | -27.20 | n/a | -27.37 | n/a | -25.00 | n/a | -25.71 | -25.46 | n/a | n/a | n/a | n/a | -25.75 |
| | 17 | n/a | n/a | -31.30 | n/a | n/a | n/a | n/a | n/a | n/a | n/a | n/a | n/a | n/a | n/a | -24.04 | n/a |
| | 18 | -33.97 | -33.90 | -34.24 | n/a | n/a | -30.50 | n/a | -28.92 | -30.45 | -29.30 | -31.18 | -30.82 | -25.88 | -25.72 | -26.06 | -27.44 |
| | 19 | n/a | n/a | n/a | n/a | n/a | n/a | n/a | n/a | n/a | n/a | n/a | n/a | n/a | n/a | n/a | n/a |
| | 20 | -30.22 | -30.77 | -29.72 | n/a | n/a | n/a | n/a | n/a | n/a | n/a | -28.89 | -28.28 | n/a | n/a | -27.01 | n/a |

Conclusions

NHOM residues were isolated from eight sediment samples and characterized via spectroscopic and molecular analyses. Solid state ^{13}C NMR results revealed the highly aliphatic nature of the NHOM residue with a smaller aromatic contribution attributed to lignin moieties, seaward from the river mouth. Further analysis using ^1H - ^{13}C HSQC NMR confirmed the predominant contributions from polymethylene moieties and also allowed the confirmation of the presence of other functional groups typical of fatty acids.

Our RuO_4 oxidation results showed that C_4 to C_{30} alkanolic acids, and C_7 to C_{27} alkanedioic acids were liberated from both the untreated sediments and the NHOM isolates, with relative contributions reaching a maximum for C_{16} and C_9 for alkanolic and alkanedioic acids, respectively. Alkanolic acids liberated from both the untreated sediment and their NHOM isolates revealed TAR values shifting from high values in the terrestrially influenced samples, to much lower values in the more marine samples. The even-to-odd CPI index, on the other hand, remained fairly constant in all NHOM isolates, suggesting a common formation pathways and selective preservation of chemically distinct macrobiopolymers enriched in aliphatic and aromatic moieties.

CSIA of the alkanolic acids produced upon RuO_4 oxidation of the untreated sediments and their NHOM isolates showed a trend of more negative $\delta^{13}\text{C}$ signatures in terrestrial samples and less negative ones in marine samples for all alkanolic acids except the C_{15} and C_{17} molecules. This trend supports the hypothesis of *in-situ* polymerization of the two acids, resulting in their incorporation into the NHOM residue (Versteegh *et al.*, 2004). The C_{15} and C_{17} bacterial biomarkers were more enriched in ^{13}C compared to all the other alkanolic acids, while also showing a seaward enrichment in ^{13}C . This result

suggests that the NHOM fraction is likely highly processed by bacteria, and that chemical composition rather than origin (terrestrial or marine) better explains the preservation and burial potential of this fraction.

More work is required to complete our understanding of the formation pathway and preservation potential of the NHOM fraction under oxic and anoxic conditions. Very little lignin-derived OM was identified in this fraction, a result that disagrees with the current general understanding of NHOM sources and cycling. Whether this result is due to the very long reaction time used to isolate the NHOM fraction (Chapter II) or to the fact that lignin-derived compounds might be more susceptible to acid hydrolysis than previously thought remains to be confirmed. Our work confirmed however that algaenan-like structures are a major contributor to NHOM, but they also raise the question of the possible multiplicity of sources for this type of compounds as terrestrial NHOM was also enriched in these types of compounds, albeit with a $\delta^{13}\text{C}$ signature reflecting a terrestrial rather than marine source.

Chapter IV

General Conclusions

Quantitative elemental and isotopic analysis (%OC, %TN, C/N ratios, $\delta^{13}\text{C}$ and $\delta^{15}\text{N}$) of the bulk OM in estuarine and lacustrine sediments, while providing insight on OM source and diagenetic state, cannot give information on overall OM reactivity. The implementation of the chemical fractionation technique outlined in Chapter 2 allowed us to generate a more complete picture of the total OM, distinguishing the labile OM (degradable in oxic and anoxic conditions) from non-hydrolyzable OM (degraded in oxic conditions) and totally refractory OM (preserved in oxic and anoxic conditions). Elemental and isotopic analysis following each successive treatment of 9 natural sediment samples allowed us to determine the relative contribution of each of the 3 main reactivity classes as well as its isotopic signature. It allowed us to probe the overall recalcitrance of the total OM and whether there are any spatial trends across a terrestrial to marine depositional transect. We see that there is an inverse relationship between the hydrolyzable and non-hydrolyzable fractions, with NHOM becoming more prominent seaward of the river mouth. The longer exposure to oxic conditions in marine environments preferentially removes the hydrolyzable OM over NHOM, thereby concentrating NHOM and increasing its relative contribution. NHOM seems to acquire its isotopic signature from its depositional setting (i.e. where the main source of depositing OM is terrestrial, NHOM has a more terrestrial signature) suggesting that recalcitrant compounds can be synthesized by both marine and terrestrial organisms and selectively preserved in the sediment. Alternatively, these compounds are synthesized *in-*

situ through condensation reactions involving either marine or terrestrial precursors (geopolymerization).

Spectroscopic and molecular analysis of the non-hydrolyzable fraction was also conducted. FTIR analysis revealed that there is a common chemical nature of NHOM isolated from all the natural samples. Enrichment in C-C and C=C bonds shows that NHOM is highly aliphatic in nature. A prominent C-O feature most likely indicates that ether cross-linkages exist between the aliphatic chains, as is common in algaenans. These findings were further supported by solid state ^{13}C and ^1H NMR.

The cross-linkages within this lipid-like material were targeted using a mild RuO_4 oxidation, liberating alkanolic ($\text{C}_4\text{-C}_{30}$ chains) and alkandioic acids ($\text{C}_7\text{-C}_{27}$ chains). The carbon preference index indicates that the organic material collected from our most marine sampling station is more diagenetically advanced than other stations along the transect. Compound-specific isotopic analysis shows that the isotopic composition of the acids liberated from NHOM is similar to the acids liberated from the bulk sample, indicating the common origin of both the bulk OM and the NHOM in these samples. Scaling up the sample size used during the oxidation to increase the yields of alkandioic acids would generate a more complete isotopic picture. Advanced statistical analysis (principal component analysis) of the isotopic signature and yield of oxidation products may also prove useful for the identification of obscured trends in our data and may expand our mechanistic understanding of preservation and synthesis of the non-hydrolyzable fraction.

Future studies should also focus on quantifying the terrestrial contribution to NHOM. Molecular analysis targeting aromatic compounds (almost exclusively

continental in origin) would reveal the chemical nature and overall input of terrestrially-derived OM. Previous studies show that very little lignin accumulates in marine sediments (Hedges & Keil, 1997), suggesting that lignin may be quickly degraded and may not be as recalcitrant as previously thought. Molecular analysis of lignin contributions to NHOM may further our understanding of preferential preservation. Additionally, radiocarbon measurements to determine the age of NHOM relative to the bulk OM in sediments, sinking particles in the water column and primary producers would help constrain the source of this OM, whether it be continental or marine and whether it was generated via selective preservation or geopolymerization. Recent studies using this proxy have determined that freshly deposited OM only makes up approximately 30% of sedimentary OM in the Arctic ocean (Goñi *et al.*, 2005), suggesting that a large reservoir of old kerogen is eroded from the continent and accumulated alongside fresher OM. Finally, repeating this study using sediments from different depositional environments (oxic and anoxic zones, high/low productivity regions, shallow lakes and the deep oceans) may allow us to find global preservation patterns and trends.

References

- Alkhatib, M., Schubert, C.J., del Giorgio, P.A., Gélinas, Y. and Lehmann, M.F. (2012) Organic matter reactivity indicators in sediments of the St. Lawrence Estuary. *Estuarine, Coastal and Shelf Sciences* (in press).
- Allard, B., Templier, J., Largeau, C., (1998) An improved method for the isolation of artifact-free algaenans from microalgae. *Organic Geochemistry*, 28(9-10), 543-548.
- Altabet, M.A., Francois, R., (1994) Sedimentary nitrogen isotopic ratio as a recorder for surface ocean nitrate utilization. *Global Biogeochem. Cycles*, 8(1), 103-116.
- Arnarson, T.S., Keil, R.G., (2007) Changes in organic matter–mineral interactions for marine sediments with varying oxygen exposure times. *Geochimica et Cosmochimica Acta*, 71(14), 3545-3556.
- Augris, N., Balesdent, J., Mariotti, A., Derenne, S., Largeau, C., (1998) Structure and origin of insoluble and non-hydrolyzable, aliphatic organic matter in a forest soil. *Organic Geochemistry*, 28(1–2), 119-124.
- Berner, R.A., (2003) The long-term carbon cycle: fossil fuel and atmospheric composition. *Nature*, 427, 323-326.
- Blokker, P., Schouten, S., van den Ende, H., de Leeuw, J.W., Hatcher, P.G., Sinnighe Damsté, J.S., (1998) Chemical structure of algaenans from the fresh water algae *Tetraedron minimum*, *Scenedesmus communis* and *Pediastrum boryanum*. *Organic Geochemistry*, 29(5-7), 1453-1468.
- Blokker, P., van den Ende, H., de Leeuw, J.W., Versteegh, G.J.M., Damsté, J.S.S., (2006) Chemical fingerprinting of algaenans using RuO₄ degradation. *Organic Geochemistry*, 37(8), 871-881.
- Bourbonniere, R.A., Meyers, P.A., (1996) Sedimentary geolipid records of historical changes in the watersheds and productivities of Lakes Ontario and Erie. *Limnology and Oceanography*, 41, 352-359.
- Burdige, D.J., (2006) *Geochemistry of marine sediments*. Princeton University Press.
- Cooper, J.E., Bray, E.E., (1963) A postulate role of fatty acids in petroleum formation. *Geochimica et Cosmochimica Acta*, 27, 1113-1127.

- Cowie, G.L., Hedges, J.I., (1992) The role of anoxia in organic matter preservation in coastal sediments: relative stabilities of the major biochemicals under oxic and anoxic depositional conditions. *Organic Geochemistry*, 19(1–3), 229-234.
- Cowie, G.L., Hedges, J.I., Prahl, F.G., De Lange, G.J., (1995) Elemental and major biochemical changes across an oxidation front in a relict turbidite: A clear-cut oxygen effect. *Geochimica et Cosmochimica Acta*, 59, 33-46.
- Derenne, S., Largeau, C., Berkaloff, C., Rousseau, B., Wilhelm, C., Hatcher, P.G., (1992) Non-hydrolysable macromolecular constituents from outer walls of *Chlorella fusca* and *Nanochlorum eucaryotum*. *Phytochemistry*, 31(6), 1923-1929.
- Dickens, A.F., Gelinas, Y., Masiello, C.A., Wakeham, S., Hedges, J.I., (2004) Reburial of fossil organic carbon in marine sediments. *Nature*, 427(6972), 336-339.
- El-Sabh, M.I., Silverberg, N., (1990) Oceanography of a Large-scale Estuarine System. Springer-Verlag New York.
- Eusterhues, K., Rumpel, C., Kögel-Knabner, I., (2007) Composition and radiocarbon age of HF-resistant soil organic matter in a Podzol and a Cambisol. *Organic Geochemistry*, 38(1356-1372).
- Fowler, S.W., Knauer, G.A., (1986) Role of large particles in the transport of elements and organic compounds through the oceanic water column. *Progress In Oceanography*, 16(3), 147-194.
- Gelin, F., Boogers, I., Noordeloos, A.A.M., Damste, J.S.S., Riegman, R., De Leeuw, J.W., (1997) Resistant biomacromolecules in marine microalgae of the classes Eustigmatophyceae and Chlorophyceae: Geochemical implications. *Organic Geochemistry*, 26(11–12), 659-675.
- Gelin, F., de Leeuw, J.W., Damsté, J.S.S., Derenne, S., Largeau, C., Metzger, P., (1994) The similarity of chemical structures of soluble aliphatic polyaldehyde and insoluble algaenan in the green microalga *Botryococcus braunii* race A as revealed by analytical pyrolysis. *Organic Geochemistry*, 21(5), 423-435.
- Gélinas, Y., Baldock, J.A., Hedges, J.I., (2001a) Organic Carbon Composition of Marine Sediments: Effect of Oxygen Exposure on Oil Generation Potential. *Science*, 294(5540), 145-148.

- Gélinas, Y., Baldock, J.A., Hedges, J.I., (2001b) Demineralization of marine and freshwater sediments for CP/MAS ¹³C NMR analysis. *Organic Geochemistry*, 32(677-693).
- Gilbert, D., Sundby, B., Gobeil, C., Mucci, A., Tremblay, G.H., (2005) A seventy-two-year record of diminishing deep-water oxygen in the St. Lawrence estuary: The northwest Atlantic connection. *Limnology and Oceanography*, 50(5), 1654-1666.
- Goñi, M.A., Yunker, M.B., Macdonald, R.W., Eglinton, T.I., (2005) The supply and preservation of ancient and modern components of organic carbon in the Canadian Beaufort Shelf of the Arctic Ocean. *Marine Chemistry*, 93(1), 53-73.
- Hartnett, H.E., Keil, R.G., Hedges, J.I., Devol, A.H., (1998) Influence of oxygen exposure time on organic carbon preservation in continental margin sediments. *Nature*, 391(6667), 572-575.
- Hayes, J.M., (1993) Factors controlling ¹³C contents of sedimentary organic compounds: Principles and evidence. *Marine Geology*, 113(1-2), 111-125.
- Hedges, J.I., Cowie, G.L., Richey, J.E., Quay, P.D., Benner, R., Strom, M., Forsberg, B.R., (1994) Origins and processing of organic matter in the Amazon River as indicated by carbohydrates and amino acids. *Limnology and Oceanography*, 39, 743-761.
- Hedges, J.I., Keil, R.G., (1995) Sedimentary organic matter preservation: an assessment and speculative synthesis. *Marine Chemistry*, 49(2-3), 81-115.
- Hedges, J.I., Keil, R.G.B., R., (1997) What happens to terrestrial organic matter in the ocean? *Organic Geochemistry*, 27, 195-212.
- Hedges, J.I., Oades, J.M., (1997) Comparative organic geochemistries of soils and marine sediments. *Organic Geochemistry*, 27, 319-361.
- Hwang, J., Druffel, E., (2003) Lipid-Like Material as the Source of the Uncharacterized Organic Carbon in the Ocean? *Science*, 299(5608), 881-884.
- Hwang, J., Druffel, E.R.M., Eglinton, T.I., Repeta, D.J., (2006) Source(s) and cycling of the nonhydrolyzable organic fraction of oceanic particles. *Geochimica et Cosmochimica Acta*, 70(20), 5162-5168.

- Kawamura, K., Ishiwatari, R., Ogura, K., (1987) Early diagenesis of organic matter in the water column and sediment: Microbial degradation and resynthesis of lipids in Lake Haruna. *Organic Geochemistry*, 11(4), 251-264.
- Keil, R.G., Montlucon, D.B., Prahl, F.G., Hedges, J.I., (1994b) Sorptive preservation of labile organic matter in marine sediments. *Nature*, 370(549-552).
- Kennedy, M.J., Wagner, T., (2011) Clay mineral continental amplifier for marine carbon sequestration in a greenhouse ocean. *Proceedings of the National Academy of Sciences*, 108(24), 9776-9781.
- Kononova, M.M., (1966) *Soil Organic Matter*. Pergamon Press, New York.
- Lalonde, K., Mucci, A., Ouellet, A., Gelinis, Y., (2012) Preservation of organic matter in sediments promoted by iron. *Nature*, 483(7388), 198-200.
- Largeau, C., Casadevall, E., Kadouri, A., Metzger, P., (1984) Formation of Botryococcus-derived kerogens—Comparative study of immature torbanites and of the extent alga Botryococcus braunii. *Organic Geochemistry*, 6(0), 327-332.
- Luthy, R.G., Aiken, G.R., Brusseau, M.L., Cunningham, S.D., Gschwend, P.M., Pignatello, J.J., Reinhard, M., Traina, S.J., Weber, W.J., Westall, J.C., (1997) Sequestration of hydrophobic contaminants by geosorbents. *Environmental Science & Technology*, 31, 3341-3347.
- Maillard, L.C., Acad, C.R., (1912) Action des acides aminés sur les sucres: formation des mélanoidines par voie méthodique. *l'Académie des sciences*(154), 66-68.
- Mathers, N.J., Jalota, R.K., Dalal, R.C., Boyd, S.E., (2007) ¹³C-NMR analysis of decomposing litter and fine roots in the semi-arid Mulga Lands of southern Queensland. *Soil Biology and Biochemistry*, 39(5), 993-1006.
- Mayer, L.M., (1994) Surface area control of organic carbon accumulation in continental shelf sediments. *Geochimica et Cosmochimica Acta*, 58(4), 1271-1284.
- Mayer, L.M., (1999) Extent of coverage of mineral surfaces by organic matter in marine sediments. *Geochimica et Cosmochimica Acta*, 63(2), 207-215.
- Mayer, L.M., Rahaim, P.T., Guerin, W., Macko, S.A., Watling, L., Anderson, F.E., (1985) Biological and granulometric controls on sedimentary organic matter of an intertidal mudflat. *Estuarine, Coastal and Shelf Science*, 20(4), 491-503.

- Mayer, L.M., Schick, L.L., Hardy, K.R., Wagai, R., McCarthy, J., (2004) Organic matter in small mesopores in sediments and soils. *Geochimica et Cosmochimica Acta*, 68, 3863-3872.
- Nguyen, R.T., Harvey, H.R., Zang, X., van Heemst, J.D.H., Hetényi, M., Hatcher, P.G., (2003) Preservation of algaenan and proteinaceous material during the oxic decay of *Botryococcus braunii* as revealed by pyrolysis-gas chromatography/mass spectrometry and ¹³C NMR spectroscopy. *Organic Geochemistry*, 34(4), 483-497.
- Nip, M., Tegelaar, E.W., Brinkhuis, H., De Leeuw, J.W., Schenck, P.A., Holloway, P.J., (1986) Analysis of modern and fossil plant cuticles by Curie point Py-GC and Curie point Py-GC-MS: Recognition of a new, highly aliphatic and resistant biopolymer. *Organic Geochemistry*, 10(4–6), 769-778.
- Orginc, N., Fontolan, G., Faganeli, J., Covelli, S., (2005) Carbon and nitrogen isotope compositions of organic matter in coastal marine sediments (the Gulf of Trieste, N Adriatic Sea): indicators of sources and preservation. *Marine Chemistry*, 95, 163-181.
- Peters, K.E., Sweeny, R.E., Kaplan, I.R., (1978) Correlation of carbon and nitrogen stable isotope ratios in sedimentary organic matter. *Limnology and Oceanography*, 23(4), 598-604.
- Peterson, B.J.H., R. W., (1978) Sulfur, carbon and nitrogen isotopes used to trace organic matter flow in salt-marsh estuaries of Sapelo Island, Georgia. *Limnology and Oceanography*, 32(6), 1195-1213.
- Prahl, F.G., de Lange, G.J., Scholten, S., Cowie, G.L., (1997) Case of post-depositional aerobic degradation of terrestrial OM in turbidite deposits from the Madeira Abyssal Plain. *Organic Geochemistry*, 27, 141-152.
- Ransom, B., Bennett, R.H., Baerwald, R., Shea, K., (1997) TEM study of in situ organic matter on continental margins: occurrence and the “monolayer” hypothesis. *Marine Geology*, 138(1–2), 1-9.
- Ransom, B., Kim, D., Kastner, M., Wainwright, S., (1998) Organic matter preservation on continental slopes: importance of mineralogy and surface area. *Geochimica et Cosmochimica Acta*, 62(8), 1329-1345.

- Rumpel, C., Rabia, N., Derenne, S., Quenea, K., Eusterhues, K., Kögel-Knabner, I., Mariotti, A., (2006) Alteration of soil organic matter following treatment with hydrofluoric acid (HF). *Organic Geochemistry*, 37(1437-1451).
- Samios, S., Lekkas, T., Nikolaou, A., Golfopoulos, S., (2007) Structural investigations of aquatic humic substances from different watersheds. *Desalination*, 210(1-3), 125-137.
- Sawyer, D.T., (1991) *Oxygen Chemistry*. Oxford University Press, New York.
- Schouten, S., Moerkerken, P., Gelin, F., Baas, M., Leeuw, J.W., Damsté, J.S.S., (1998) Structural characterization of aliphatic, non-hydrolyzable biopolymers in freshwater algae and a leaf cuticle using ruthenium tetroxide degradation. *Phytochemistry*, 49(4), 987-993.
- Simpson, A.J., Simpson, M.J., Smith, E., Kelleher, B.P., (2007) Microbially Derived Inputs to Soil Organic Matter: Are Current Estimates Too Low? *Environmental Science & Technology*, 41(23), 8070-8076.
- Simpson, A.J., Zang, X., Kramer, R., Hatcher, P.G., (2003) New insights on the structure of algaenan from *Botryococcus braunii* race A and its hexane insoluble botryals based on multidimensional NMR spectroscopy and electrospray-mass spectrometry techniques. *Phytochemistry*, 62(5), 783-796.
- Smith, J.N., Schafer, C.T., (1999) Sedimentation, Bioturbation, and Hg Uptake in the Sediments of the Estuary and Gulf of St. Lawrence. *Limnology and Oceanography*, 44(1), 207-219.
- Tegelaar, E.W., de Leeuw, J.W., Derenne, S., Largeau, C., (1989b) A reappraisal of kerogen formation. *Geochimica et Cosmochimica Acta*, 53(11), 3103-3106.
- Tegelaar, E.W., de Leeuw, J.W., Saiz-Jimenez, C., (1989c) Possible origin of aliphatic moieties in humic substances. *Science of The Total Environment*, 81-82(0), 1-17.
- Tegelaar, E.W., Matthezing, R.M., Jansen, J.B.H., Horsfield, B., de Leeuw, J.W., (1989a) Possible origin of n-alkanes in high-wax crude oils. *Nature*, 342(6249), 529-531.
- Treibs, A.E., (1936) Chlorophyll and hemin derivatives in organic mineral substances. *Angewandte Chemie*, 49, 682-686.

- Tremblay, L., Benner, R., (2006) Microbial contributions to N-immobilization and organic matter preservation in decaying plant detritus. *Geochimica et Cosmochimica Acta*, 70(1), 133-146.
- Vandenbroucke, M., Largeau, C., (2007) Kerogen origin, evolution and structure. *Organic Geochemistry*, 38(5), 719-833.
- Versteegh, G.J.M., Blokker, P., Wood, G.D., Collinson, M.E., Sinninghe Damsté, J.S., de Leeuw, J.W., (2004) An example of oxidative polymerization of unsaturated fatty acids as a preservation pathway for dinoflagellate organic matter. *Organic Geochemistry*, 35(10), 1129-1139.
- Wagai, R., Mayer, L.M., (2007) Sorptive stabilization of organic matter in soils by hydrous iron oxides. *Geochimica et Cosmochimica Acta*, 71(1), 25-35.
- Yoshioka, H., Ishiwatari, R., (2005) An improved ruthenium tetroxide oxidation of marine and lacustrine kerogens: possible origin of low molecular weight acids and benzenecarboxylic acids. *Organic Geochemistry*, 36(1), 83-94.